Materials and Methods

Primary human cells

Blood samples were obtained from healthy volunteers, HTLV-1 asymptomatic carriers (ACs), and ATL patients. Mononuclear cells were isolated with Ficoll-Paque (Pharmacia, Peapack, NJ). Genotyping of HLA-DR, HLA-DQ, and HLA-DP was performed using an WAKFlow HLA-typing kit (WAKUNAGA Pharmacy, Hiroshima, Japan). Diagnosis and classification of clinical subtypes of ATL were according to the criteria proposed by the Japan Lymphoma Study Group (32). All donors provided informed written consent before sampling, according to the Declaration of Helsinki, and the current study was approved by the institutional ethics committees of Nagoya City University Graduate School of Medical Sciences.

Cell lines

ATN-1, MT-1, TL-Om1, and ATL102 are ATL cell lines; MT-2, MT-4, and TL-Su are HTLV-1–immortalized lines; and K562 is a chronic myelogenous leukemia blast crisis cell line (8, 33). Genotyping of HLA-DR, HLA-DQ, and HAL-DP was performed using a WAKFlow HLA-typing kit.

Expansion of HBZ-specific T cells

PBMCs from ATL patients or HTLV-1 ACs were suspended in RPMI 1640 (Cell Science and Technology Institute, Sendai, Japan) supplemented with 10% human serum and 10 μM synthetic HBZ-derived peptides at a cell concentration of 2×10^6/ml. The peptides were purchased from Invitrogen (Carlsbad, CA). The cell suspension (2×10^6 cells) was cultured at 37°C in 5% CO_2 for 2 d, and an equal volume of RPMI 1640 supplemented with 100 IU/ml IL-2 was added. After subsequent culture for 5 d, an equal volume of ALyS505N (Cell Science and Technology Institute) supplemented with 100 IU/ml IL-2 was added, and the cells were cultured with appropriate medium (ALyS505N with 100 IU/ml IL-2) for an additional 7 d.

Abs and flow cytometry

PerCP-conjugated anti-CD8 mAb (SK1; eBioscience, San Diego, CA) and PE-conjugated anti-CD4 mAb [SFCI12T4D11 (T4); Beckman Coulter, Fullerton, CA] were used. For assessing HLA class II expression, PE-conjugated anti–HLA-DR (G46-6; BD Biosciences, San Jose, CA), anti–HLA-DQ (HLA-DQ1; BioLegend, San Diego, CA), or appropriate isotype-control mAbs were used. For intracellular IFN-γ and TNF-α staining, the expanded cells were cocultured with or without target cells or synthetic peptides at 37°C in 5% CO_2 for 3 h, after which brefeldin A (BD Biosciences) was added at 2 μg/ml. The cells were then incubated for an additional 2 h. Subsequently, they were fixed in 10% formaldehyde and stained with FITC-conjugated anti–IFN-γ (45.15; Beckman Coulter) or allophycocyanin-conjugated anti–TNF-α (MAb11; eBioscience) mAbs with 0.25% saponin for 60 min at room temperature. To determine HLA restriction, HLA-blocking experiments were conducted. The expanded cells were preincubated with 20 μg/ml anti–HLA-DR (L243; BioLegend), 20 μg/ml anti–HLA-DQ (1SPVL3; Beckman Coulter), or appropriate isotype control mAbs (20 μg/ml) at 37°C in 5% CO_2 for 1 h, after which they were stimulated with the peptide or the cell lines (ATN-1 and K562). Cells were analyzed on a FACSCalibur (BD Biosciences) with the aid of FlowJo software (Tree Star, Ashland, OR).

Quantitative RT-PCR

Total RNA was isolated with RNeasy Mini Kits (QIAGEN, Tokyo, Japan). Reverse transcription from the RNA to first-strand cDNA was carried out using High Capacity RNA-to-cDNA Kits (Applied Biosystems, Foster City, CA). *HBZ* and *β-actin* mRNA were amplified using TaqMan Gene Expression Assays with the aid of an Applied Biosystems StepOnePlus. The primer set for *HBZ* was as follows: sense, 5′-TCGACCTGAGCTTTAAACTTACCTAGA-3′ and antisense, 5′-GACACAGGCAAGCATCGAAA-3′. All values given are means of triplicate determinations.

Results

T cell responses against synthetic peptides overlapping by 10 aa and covering the entire sequence of the spliced HBZ protein

Because it was reported that HTLV-1 Tax-specific T cells were induced in some ATL patients after allogeneic HCT (10, 11), we initially tried to expand HBZ-specific T cells using PBMCs from an ATL patient who received allogeneic HCT with reduced-intensity conditioning and has been in complete remission (CR) for >3 y (patient #1 after HCT). PBMCs were stimulated with a mixture of 1 16-mer and 19 20-mer synthetic peptides overlapping by 10 aa and covering the entire sequence of the spliced HBZ protein (peptides number 1–20, Fig. 1), at a concentration of 10 μM each. The expanded cells were analyzed by forward scatter height and side scatter height levels, and the lymphocyte population was determined and plotted to show CD4 and CD8 positivity (Fig. 2A, *left panels*). The expanded CD8 T cells responded weakly to stimulation with these 20 overlapping peptides relative to controls without peptide stimulation, as assessed by IFN-γ production (Fig. 2A, *upper middle panels*) but not TNF-α (Fig. 2A, *lower middle panels*). In contrast, the expanded CD4 T cells responded to stimulation by the 20 overlapping peptides by producing both IFN-γ (Fig. 2A, *upper right panels*) and TNF-α (Fig. 2A, *lower right panels*). Because the response of the stimulated and expanded CD4 T cells was stronger than the CD8 response, we focused on the CD4 T cell response against HBZ in patient #1 after HCT.

PBMCs from this patient (#1 after HCT) were stimulated with a mixture of five overlapping peptides consisting of peptides 1–4, 5–8, 9–12, 13–16, and 17–20 (Fig. 1). The expanded CD4 T cells responded to the peptide mixture 9–12 better than to control (no peptides). They produced both IFN-γ (Fig. 2B, *upper panels*) and TNF-α (Fig. 2B, *lower panels*). The expanded CD4 T cells responded very weakly to the peptide mixtures 13–16 and 17–20 by producing TNF-α but not IFN-γ. No responses were observed against the peptide mixtures 1–4 or 5–8 (Fig. 2B). These data indicate that the epitope of HBZ recognized by CD4 T cells from the patient was present in peptides 9–12, within HBZ aa residues 81–130 (Fig. 1).

Next, PBMCs from the same patient were stimulated with four synthetic peptides: 9, 10, 11, and 12. The expanded CD4 T cells responded to peptide 12 by producing both IFN-γ (Fig. 2C, *upper panels*) and TNF-α (Fig. 2C, *lower panels*). The cells did not respond significantly to the other peptides (9, 10, or 11). These results narrow down the specific epitope of HBZ recognized by the CD4 T cells from the patient to a sequence within peptide 12: HBZ aa 111–130 (Fig. 1).

Determination of the minimum epitope sequence of HBZ recognized by CD4 T cells

Seven synthetic peptides (12-1, 12-2, 12-3, 12-4, 12-5, 12-6, 12-7) representing parts of peptide 12 were prepared (Fig. 3A). Responses of the CD4 T cells, which had been stimulated by peptide 12, to these different peptides were tested. The expanded CD4 T cells responded better to peptides 12, 12-1, 12-2, 12-3, and 12-4

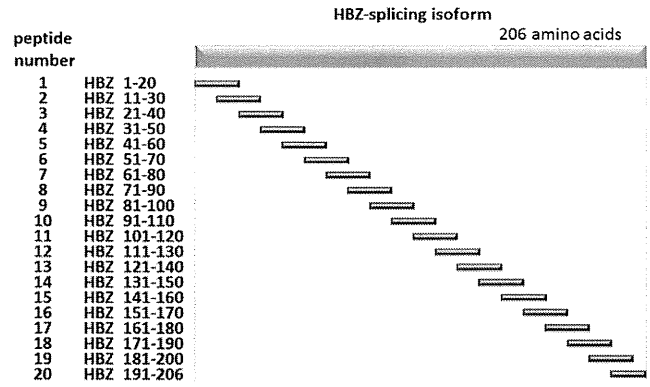

FIGURE 1. Synthetic peptides derived from spliced HBZ. Schematic of 19 20-mer and 1 16-mer synthetic peptides overlapping by 10 aa and covering the entire sequence of the spliced HBZ protein.

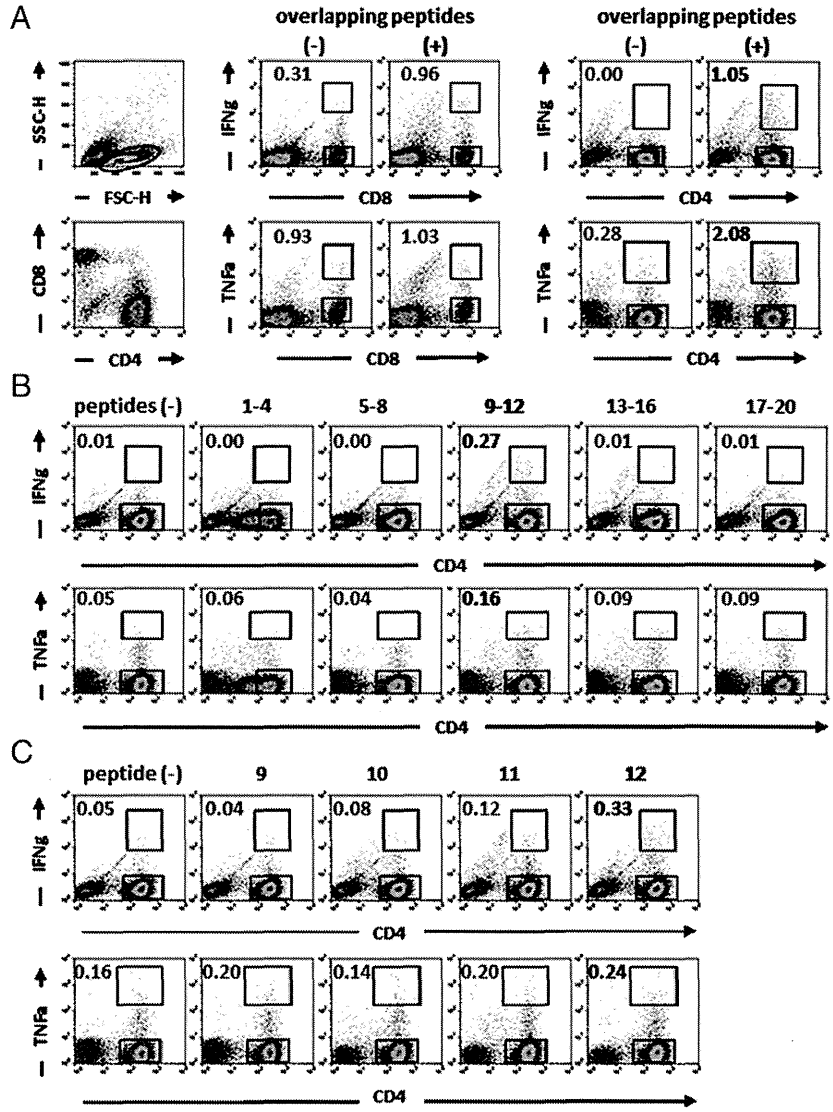

FIGURE 2. T cell responses against synthetic peptides overlapping by 10 aa and covering the entire sequence of the spliced HBZ protein. (**A**) PBMCs from patient #1 after HCT were expanded by stimulating with a mixture of 19 20-mer and 1 16-mer synthetic peptides overlapping by 10 aa and covering the entire sequence of the spliced HBZ protein. The responses of expanded CD8 and CD4 T cells to each of the overlapping peptides were evaluated by the production of IFN-γ or TNF-α. The percentage of responding cells in the upper gate ($CD8^+$ or $CD4^+$ and IFN-γ^+ or TNF-α^+ cells) relative to the cells in the lower gate ($CD8^+$ or $CD4^+$ and IFN-γ^- or TNF-α^- cells) is indicated in each flow cytometry panel. (**B**) PBMCs from patient #1 after HCT were expanded by stimulating with five overlapping peptide mixtures consisting of peptides 1–4, 5–8, 9–12, 13–16, and 17–20. (**C**) PBMCs from patient #1 after HCT were expanded by stimulating with four synthetic peptides: 9, 10, 11, and 12. The responses of expanded CD4 T cells to each synthetic peptide were evaluated by the production of IFN-γ or TNF-α. The percentage of responding cells in the upper gate relative to the cells in the lower gate is indicated in each flow cytometry panel. Each result is representative of three independent experiments.

by producing both IFN-γ and TNF-α. These cells did not respond to peptides 12-5, 12-6, or 12-7 (Fig. 3B). These data indicate that the N terminus of the minimum epitope sequence of HBZ recognized by the CD4 T cells from the patient is arginine, located at HBZ114 (Fig. 3A). Because the expanded CD4 T cells responded to peptide 12-4, the C terminus of the minimum epitope sequence of HBZ must be inside of alanine, located at HBZ125.

Next, three synthetic peptides (12-4-1, 12-4-2, 12-4-3; sequences were HBZ114–124, HBZ114–123, and HBZ114–122, respectively) were prepared to determine the C terminus of the minimum epitope sequence of HBZ (Fig. 3C). The expanded CD4 T cells responded to peptides 12-1 and 12-4 (positive controls) but not to 12-4-1, 12-4-2, 12-4-3, or a negative control peptide 12-7 (Fig. 3D). These data demonstrate that the minimum epitope sequence of HBZ recognized by the CD4 T cells from the patient was RRRAEKKAADVA (HBZ114–125).

Determination of the HLA allele on which the identified HBZ-derived peptides are presented to CD4 T cells

We investigated whether HBZ-specific CD4 T cells also recognized naturally processed and presented peptides. Thus, we initially determined *HBZ* expression by ATL or HTLV-1–immortalized cell lines and found that it was expressed by all of the lines tested (ATN-1, MT-1, MT-2, MT-4, TL-Su, TL-Om1, ATL102), regardless of their *Tax* mRNA expression (Fig. 4A, below the graph). *HBZ* expression levels of these established lines were almost as high as those of PBMCs containing >50% ATL cells obtained from 12 patients with the acute or chronic type of disease. K562 did not express *HBZ*, as might be expected, and all primary ATL cells tested were HBZ^+, consistent with an earlier study (Fig. 4A) (25). Next, we assessed the expression of HLA class II by the cell lines. The ATL or HTLV-1–immortalized cell lines tested were all positive for both HLA-DR and HLA-DQ (Fig. 4B). These observations indicate that ATN-1, MT-1, MT-2, MT-4, TL-Su, TL-Om1, and ATL102 had the potential to present the HBZ-derived peptides on their HLA-DR or HLA-DQ molecules.

Next, we examined the responses of HBZ-specific CD4 T cells from patient #1 after HCT against K562 or HBZ-expressing lines of different HLA types. The responses of HBZ-specific CD4 T cells to the lines were evaluated without the addition of peptide. The CD4 T cells that had been expanded from patient #1 after HCT using peptide 12 responded to peptide 12-1 (positive control) but not to K562, which expressed no *HBZ* (negative control) (Fig. 4C, *upper six panels*). When tested against ATL or HTLV-1–immortalized cell lines, the CD4 T cells responded strongly to ATN-1 and TL-Su (Fig. 4C, *lower panels*). Comparing the HLA class II types of the donor of the effector CD4 T cells (patient #1 after HCT) with ATN-1 and TL-Su showed that HLA-DRB1*15:01 and

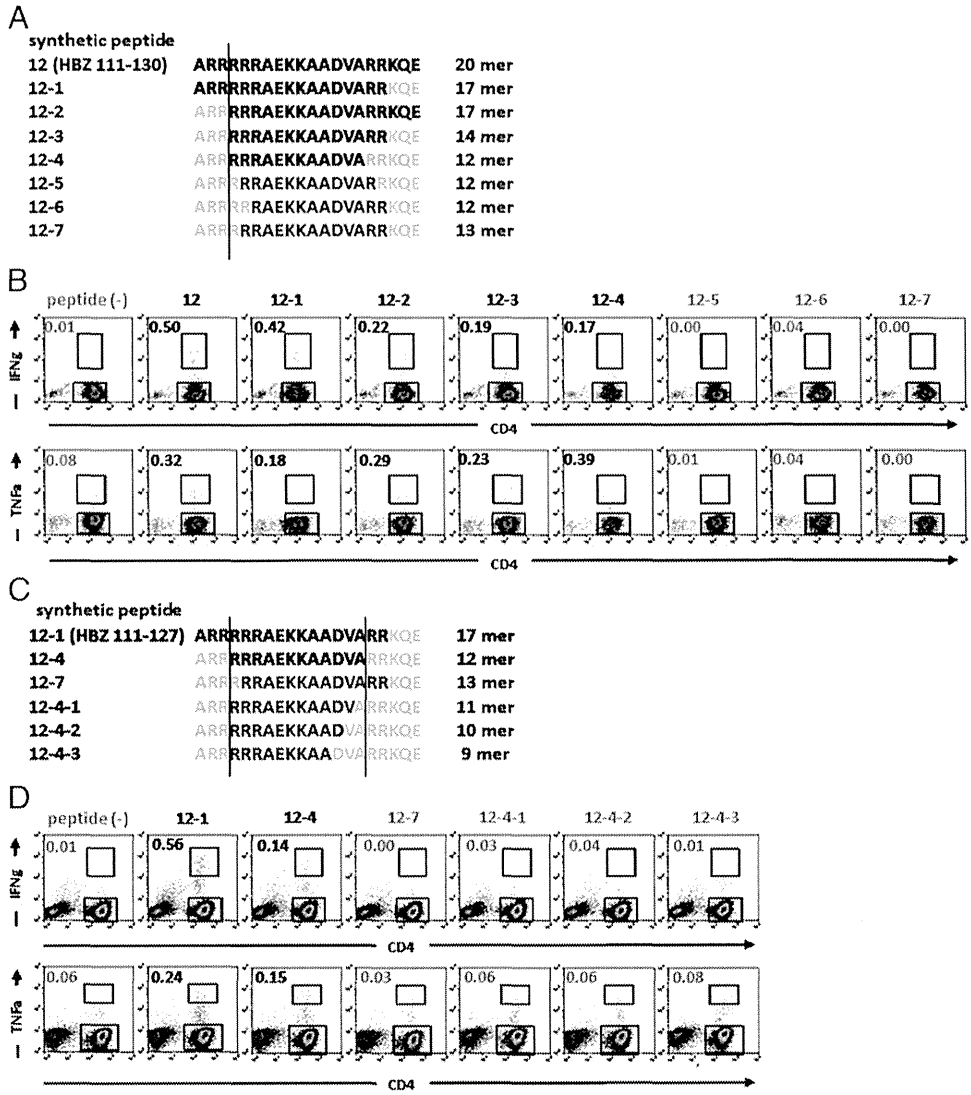

FIGURE 3. Determination of the minimum epitope sequence of HBZ recognized by CD4 T cells. (**A**) Schematic diagram of seven synthetic peptides (12-1, 12-2, 12-3, 12-4, 12-5, 12-6, 12-7) from peptide 12. They were prepared to determine the N terminus of the sequence representing the minimum epitope of HBZ recognized by the CD4 T cells. (**B**) PBMCs from patient #1 after HCT were expanded by peptide 12. The responses of expanded CD4 T cells to each synthetic peptide (12, 12-1, 12-2, 12-3, 12-4, 12-5, 12-6, 12-7) were evaluated by the production of IFN-γ or TNF-α. The percentage of responding cells in the upper gate relative to the cells in the lower gate is indicated in each flow cytometry panel. Each result is representative of three independent experiments. (**C**) Schematic diagram of three synthetic peptides (12-4-1, 12-4-2, 12-4-3) prepared to determine the C terminus of the sequence representing the minimum epitope of HBZ recognized by the CD4 T cells. (**D**) The responses of expanded CD4 T cells to each synthetic peptide (12-1, 12-4, 12-7, 12-4-1, 12-4-2, 12-4-3) were evaluated by the production of IFN-γ or TNF-α. The percentage of responding cells in the upper gate relative to the cells in the lower gate is indicated in each flow cytometry panel. Each result is representative of three independent experiments.

HLA-DQB1*06:02 were shared by all three (Table I). In addition, the CD4 T cells responded to MT-2, TL-Om1, and ATL102 to a lesser degree (Fig. 4C, *lower panels*); these three lines were found to share HLA-DRB1*15:02 and HLA-DQB1*06:01 (Table I). Together, these results indicate that the HBZ-specific CD4 T cell responses from patient #1 after HCT were restricted by HLA-DRB1*15:01 or HLA-DQB1*06:02, as well as by HLA-DRB1*15:02 or HLA-DQB1*06:01. In contrast, the peptide-sensitized CD4 T cells did not respond to MT-1 or MT-4 (Fig. 4C, *lower panels*), consistent with the present observations that the epitope of HBZ recognized by such CD4 T cells was restricted by HLA-DRB1*15:01/HLA-DQB1*06:02 and HLA-DRB1*15:02/HLA-DQB1*06:01.

Next, we tested whether HLA-DR or HLA-DQ restricted the presentation of the HBZ-derived peptide. CD4 T cells expanded by peptide 12 no longer responded to specific stimulation by peptide 12 in the presence of anti–HLA-DR–blocking mAb by producing IFN-γ (Fig. 5A, *upper left panels*), but it did respond in the presence of the isotype-control mAb (Fig. 5A, *upper right panels*). These CD4 T cells also still responded to peptide 12 in the presence of anti–HLA-DQ–blocking mAb (Fig. 5A, *lower left panels*) and its isotype control (Fig. 5A, *lower right panels*). In addition, in the presence of anti–HLA-DR–blocking mAb, CD4 T cells expanded by peptide 12 no longer responded to ATN-1 (Fig. 5B, *left panels*), which carried HLA-DRB1*15:01/HLA-DQB1*06:02 (Table I) and expressed *HBZ* mRNA (Fig. 4A). However, they did respond by producing IFN-γ and TNF-α in the presence of the isotype control (Fig. 5B, *left panels*). These CD4 T cells also still responded to ATN-1 in the presence of anti–HLA-DQ–blocking mAb and its isotype control (Fig. 5B, *right panels*). Furthermore, HBZ-specific CD4 T cell responses to K562 (negative control) were not affected by anti–HLA-DR, anti–HLA-DQ, or their isotype mAbs (Fig. 5C). These observations from Ab-blocking experiments, together with the results shown in Fig. 4, indicate that the epitope sequence of HBZ recognized by the CD4 T cells from patient #1 after HCT were restricted by HLA-DR, specifically HLA-DRB1*15:01 and HLA-DRB1*15:02.

Clinical significance of the specific CD4 T cell response against HBZ

The data presented thus far pertained to CD4 T cells obtained from only one patient (patient #1 after HCT). Therefore, we used HBZ peptide 12 to stimulate and expand 28 PBMC samples obtained from 27 other HTLV-1–infected individuals who carried HLA-DRB1*15:01 or HLA-DRB1*15:02. PBMCs were obtained from 10 HTLV-1 ACs, 10 ATL patients who had not undergone allogeneic HCT, and 8 ATL patients after allogeneic HCT. Among them, PBMCs from one individual (patient #2) were tested at different disease stages (i.e., CRs before and after allogeneic HCT). HBZ-specific CD4 T cell responses were absent in all 10

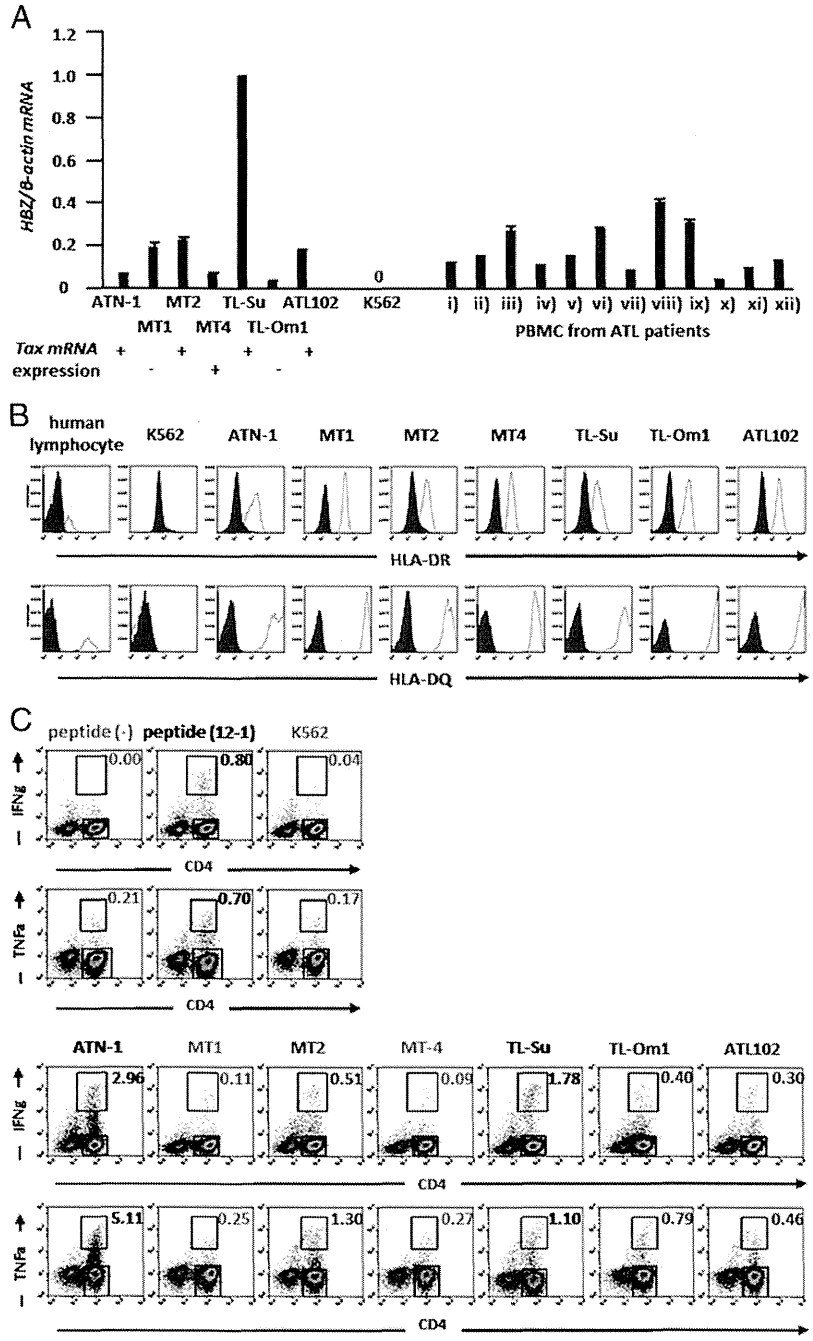

FIGURE 4. Responses of HBZ-specific CD4 T cells from patient #1 after HCT to ATL or HTLV-1–immortalized cell lines. (**A**) *HBZ* expression in ATL and HTLV-1–immortalized cell lines, K562, or PBMCs from ATL patients was analyzed by qRT-PCR by dividing the *HBZ* expression level by the *β-actin* expression level, resulting in an *HBZ/β-actin* mRNA ratio with the expression level in TL-Su set at unity. Data shown are means of triplicate experiments; error bars represent SD. *Tax* mRNA expression of each ATL and HTLV-1–immortalized cell line is indicated, as determined in our previous study (8). (**B**) HLA-DR and HLA-DQ expression in ATL cell lines, HTLV-1–immortalized lines, or K562, as analyzed by flow cytometry. The cell lines were stained with anti–HLA-DR mAb (*upper panels*, open graphs), anti–HLA-DQ mAb (*lower panels*, open graphs), or the corresponding isotype-control mAbs (filled graphs). (**C**) The expanded CD4 T cells were cocultured or not with the synthetic peptide 12-1. Negative controls without peptide stimulation (*upper left panels*) and positive controls with peptide stimulation (*upper middle panels*) are shown. The expanded CD4 T cells were cocultured with target cell lines in the absence of peptide stimulation. CD4 T cells did not respond to K562, which expressed no HBZ and acted as the negative control (*upper right panels*). The CD4 T cell responses to ATL or HTLV-1–immortalized cell lines, which expressed *HBZ*, with different HLA types were evaluated (*lower panels*). The percentage of responding cells in the upper gate relative to the cells in the lower gate is indicated in each flow cytometry panel. Each result is representative of three independent experiments.

HTLV-1 ACs, as well as in all 10 nontransplanted ATL patients (of whom 9 were in CR after systemic chemotherapy and the other was of smoldering type under observation only). In contrast, specific CD4 T cell responses to HBZ were observed in three of the eight additional ATL patients who were in CR after allogeneic HCT (patients #2, #3, and #4). The CD4 T cells from patient #2 and #4 after HCT responded to HBZ peptide 12 by producing both IFN-γ and TNF-α (Fig. 6, *right panels*). In patient #3, no TNF-α response was observed, but there was a clear IFN-γ response to HBZ peptide 12 (Fig. 6, *lower left panels*). Thus, specific CD4 T cell responses against HBZ were observed in four of nine recipients after allogeneic HCT (44%) but in no other ATL patients. Among the patients examined in this study, one patient with acute-type ATL received systemic chemotherapy and achieved CR. Subsequently, she received allogeneic HCT from an HLA-A, B, DR-matched HTLV-1 noninfected sibling donor and maintained CR (patient #2 after HCT). Although HBZ-specific CD4 T cell responses were not present at CR before allogeneic HCT in this patient (Fig. 6, *upper left panels*), they developed after transplantation (Fig. 6, *upper right panels*).

Table I. HLA information

	HLA-DRB1		HLA-DQB1		HLA-DPB1	
ATN-1	*04:05	*15:01	*04:01	*06:02	*05:01	*05:01
MT-1	*04:01	*09:01	*03:01	*03:03	*04:02	*05:01
MT-2	*04:04	*15:02	*03:02	*06:01	*05:01	*09:01
MT-4	*01:01	*16:02	*05:01	*05:02	*05:01	*05:01
TL-Su	*09:01	*15:01	*03:03	*06:02	*02:01	*17:01
TL-Om1	*15:02	*15:02	*06:01	*06:01	*09:01	*09:01
ATL102	*04:04	*15:02	*03:02	*06:01	*05:01	*09:01
Patient #1 after HCT	*04:05	*15:01	*04:01	*06:02	*02:01	*06:01

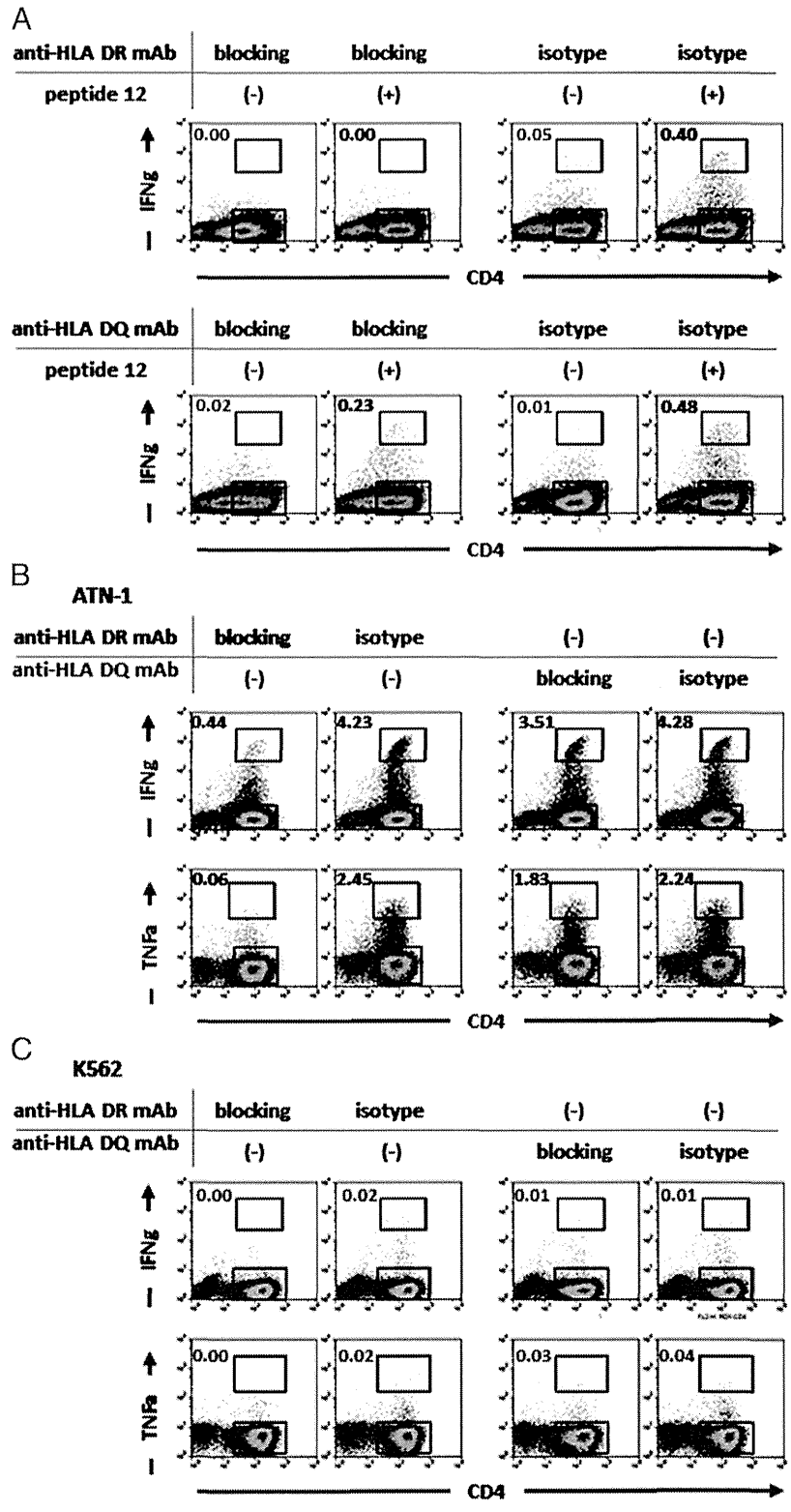

FIGURE 5. Determination of the HLA alleles restricting the presentation of HBZ-derived peptides to HBZ-specific CD4 T cells. (**A**) Responses of HBZ-specific CD4 T cells were evaluated, with or without HBZ peptide 12, in the presence of anti–HLA-DR–blocking mAb (*upper left panels*), anti–HLA-DQ–blocking mAb (*lower left panels*), or the corresponding isotype-control mAb (anti-HLA-DR isotype mAb, *upper right panels*; anti-HLA-DQ isotype mAb, *lower right panels*). Responses of HBZ-specific CD4 T cells to ATN-1, which carries HLA-DRB1*15:01/HLA-DQB1*06:02 and expresses *HBZ* mRNA (**B**), and to K562 (negative control) (**C**) were also evaluated in the presence of HLA-blocking mAbs or their isotype controls, without peptide stimulation. The percentage of responding cells in the upper gate relative to the cells in the lower gate is indicated in each flow cytometry panel. Each result is representative of three independent experiments.

Discussion

In the current study, we demonstrated the presence of HBZ-specific CD4 T cells in an ATL patient after allogeneic HCT and determined the minimum sequence of a novel HLA-DRB1*15:01–restricted HBZ-derived epitope to be RRRAEKKAADVA (HBZ114–125). HBZ peptides including the sequence HBZ114–125 were also presented on HLA-DRB1*15:02 and recognized by CD4 T cells. To the best of our knowledge, this is the first report to identify naturally processed and presented HLA-DR–restricted epitopes derived from HBZ on the surface of ATL cells. In an earlier study, an HBZ peptide–specific CTL line was established from an HLA-A*02:01^{+} individual, using peptides derived from the HBZ sequence. The peptides were selected by computer algorithms available at the BioInformatics and Molecular Analysis Section Web site (http://www-bimas.cit.nih.gov/molbio/hla_bind/) and the SYFPEITHI Web site (http://www.syfpeithi.de/) for strong binding affinity to the HLA-A*02:01 molecule. However, the established CTL line recognized the corresponding peptide-pulsed

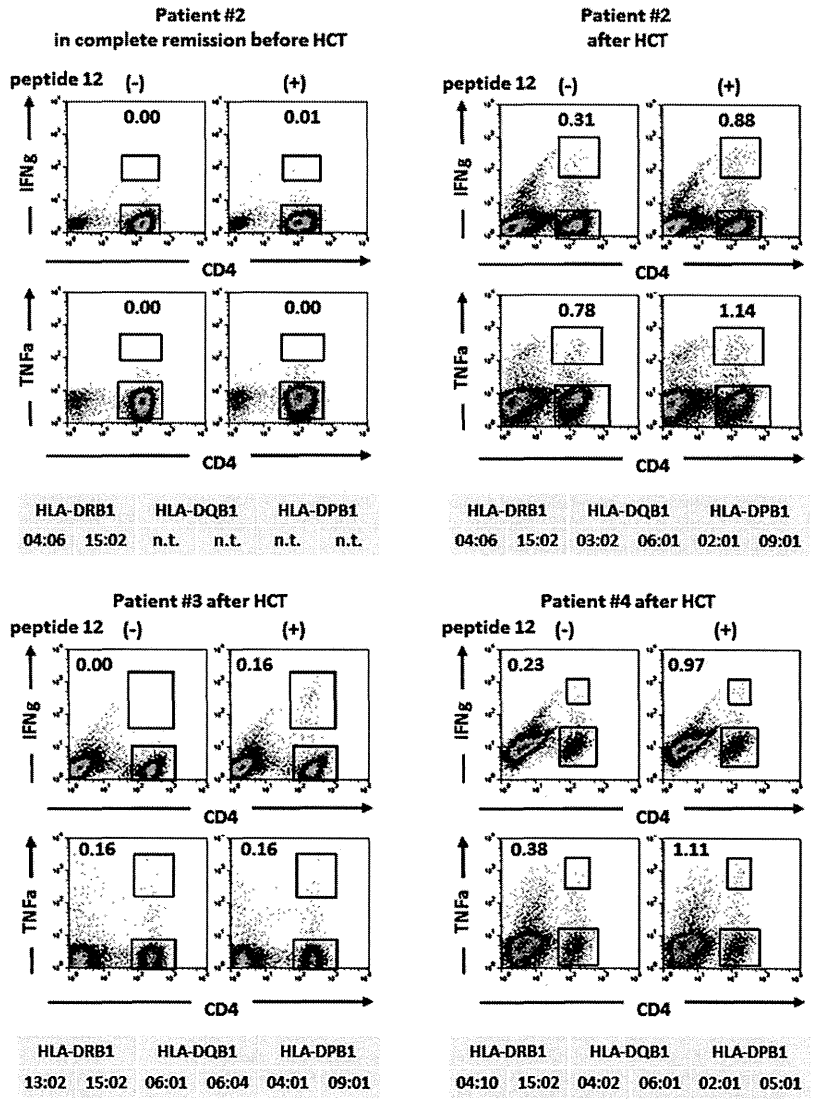

FIGURE 6. HBZ-specific CD4 T cell responses in additional ATL patients. PBMCs from additional ATL patients (#2, #3, and #4) carrying HLA-DRB1*15:02 were expanded by stimulation with HBZ peptide 12. The responses of expanded CD4 T cells to peptide 12 were evaluated by the production of IFN-γ or TNF-α. Although no HBZ-specific CD4 T cell response was observed in patient #2 in CR before allogeneic HCT (*upper left panels*), they developed after transplantation (*upper right panels*). HBZ-specific CD4 T cell responses were also observed in patient #3 (*lower left panels*) and patient #4 (*lower right panels*) in CR after allogeneic HCT. The percentage of responding cells in the upper gate relative to the cells in the lower gate is indicated in each flow cytometry panel. The HLA type of each patient is indicated below the flow cytometry panels. Each result is representative of three independent experiments. n.t., Not tested.

HLA-A*02:01$^+$ cells but not ATL cells (29). Therefore, it was not determined whether HBZ-derived peptides could be naturally presented on cells from HTLV-1–infected people. Another earlier study (30) demonstrated that HBZ expression was a critical determinant of viral persistence in the chronic phase of HTLV-1 infection. That novel study was performed using experimentally validated epitope-prediction software (34), but it did not determine the HBZ-derived epitope sequence or the corresponding HLA allele presenting it.

In the current study, no HLA-DRB1*15:01–restricted or HLA-DRB1*15:02–restricted HBZ-specific CD4 T cell response was observed in any ATL patients who had not undergone allogeneic HCT or in any HTLV-1 ACs. We surmise that HTLV-1 transmission from mothers to infants through breast milk in early life induces tolerance to HBZ, but not to Tax, by unknown mechanisms, resulting in insufficient HBZ-specific T cell responses in HTLV-1–infected individuals. This would be consistent with the persistent expression of HBZ in HTLV-1–infected cells (2, 25). In addition, insufficient HBZ-specific T cell responses may be due, in part, to the fact that the majority of the *HBZ* mRNA is retained in the nucleus, which may inhibit its translation (35), and probably leads to a low level of HBZ protein expression in HTLV-1–infected cells (29). In contrast, the finding that HLA-DRB1*15:01–restricted or HLA-DRB1*15:02–restricted HBZ-specific CD4 T cell responses were detected in ATL patients after allogeneic HCT requires explanation. Our hypothesis is that, after allogeneic HCT, the reconstituted immune system from donor-derived hematopoietic stem cells can recognize virus protein HBZ as foreign, although its expression is low, and HBZ-specific immune responses are provoked because of the lack of tolerance induction under these circumstances. In one patient with acute-type disease, HBZ-specific CD4 T cell responses were not observed in PBMCs at the time of CR before HCT, but they became detectable after allogeneic HCT. This observation supports our hypothesis. An earlier study (36) reported that HBZ-specific T cell responses were detected in some patients with HTLV-1–associated myelopathy (HAM). Unlike ATL, HAM can occur in individuals infected with HTLV-1 by any route of transmission, such as sexual intercourse (37). Therefore, some patients with HAM, infected with HTLV-1 after reaching adulthood (i.e., who became infected after their immune system had fully matured), may recognize virus protein HBZ as foreign, and HBZ-specific immune responses may be provoked. From this point of view, detection of HBZ-specific T cell responses might be expected in some HTLV-1 ACs, infected after becoming adults, but we did not see this in the present study.

In conclusion, we report the presence of HBZ-specific CD4 T cell responses in ATL patients who were in CR but only after allogeneic HCT. These responses potentially contribute to the

graft-versus-HTLV-1 effect. Novel strategies that enhance the posttransplantation allogeneic anti–HTLV-1 effect targeting HBZ, which never provokes graft-versus-host disease, could lead to improved outcomes of allogeneic HCT for ATL.

Acknowledgments

We thank Chiori Fukuyama for excellent technical assistance and Naomi Ochiai for excellent secretarial assistance.

Disclosures

T.I. received honoraria from Kyowa Hakko Kirin. The other authors have no financial conflicts of interest.

References

1. Uchiyama, T., J. Yodoi, K. Sagawa, K. Takatsuki, and H. Uchino. 1977. Adult T-cell leukemia: clinical and hematologic features of 16 cases. *Blood* 50: 481–492.
2. Matsuoka, M., and K. T. Jeang. 2007. Human T-cell leukaemia virus type 1 (HTLV-1) infectivity and cellular transformation. *Nat. Rev. Cancer* 7: 270–280.
3. Ishida, T., and R. Ueda. 2011. Antibody therapy for Adult T-cell leukemia-lymphoma. *Int. J. Hematol.* 94: 443–452.
4. Tsukasaki, K., T. Maeda, K. Arimura, J. Taguchi, T. Fukushima, Y. Miyazaki, Y. Moriuchi, K. Kuriyama, Y. Yamada, and M. Tomonaga. 1999. Poor outcome of autologous stem cell transplantation for adult T cell leukemia/lymphoma: a case report and review of the literature. *Bone Marrow Transplant.* 23: 87–89.
5. Utsunomiya, A., Y. Miyazaki, Y. Takatsuka, S. Hanada, K. Uozumi, S. Yashiki, M. Tara, F. Kawano, Y. Saburi, H. Kikuchi, et al. 2001. Improved outcome of adult T cell leukemia/lymphoma with allogeneic hematopoietic stem cell transplantation. *Bone Marrow Transplant.* 27: 15–20.
6. Ishida, T., M. Hishizawa, K. Kato, R. Tanosaki, T. Fukuda, S. Taniguchi, T. Eto, Y. Takatsuka, Y. Miyazaki, Y. Moriuchi, et al. 2012. Allogeneic hematopoietic stem cell transplantation for adult T-cell leukemia-lymphoma with special emphasis on preconditioning regimen: a nationwide retrospective study. *Blood* 120: 1734–1741.
7. Akimoto, M., T. Kozako, T. Sawada, K. Matsushita, A. Ozaki, H. Hamada, H. Kawada, M. Yoshimitsu, M. Tokunaga, K. Haraguchi, et al. 2007. Anti-HTLV-1 tax antibody and tax-specific cytotoxic T lymphocyte are associated with a reduction in HTLV-1 proviral load in asymptomatic carriers. *J. Med. Virol.* 79: 977–986.
8. Suzuki, S., A. Masaki, T. Ishida, A. Ito, F. Mori, F. Sato, T. Narita, M. Ri, S. Kusumoto, H. Komatsu, et al. 2012. Tax is a potential molecular target for immunotherapy of adult T-cell leukemia/lymphoma. *Cancer Sci.* 103: 1764–1773.
9. Masaki, A., T. Ishida, S. Suzuki, A. Ito, F. Mori, F. Sato, T. Narita, T. Yamada, M. Ri, S. Kusumoto, et al. 2013. Autologous Tax-specific CTL therapy in a primary adult T cell leukemia/lymphoma cell-bearing NOD/Shi-scid, IL-2Rγnull mouse model. *J. Immunol.* 191: 135–144.
10. Harashima, N., K. Kurihara, A. Utsunomiya, R. Tanosaki, S. Hanabuchi, M. Masuda, T. Ohashi, F. Fukui, A. Hasegawa, T. Masuda, et al. 2004. Graft-versus-Tax response in adult T-cell leukemia patients after hematopoietic stem cell transplantation. *Cancer Res.* 64: 391–399.
11. Tamai, Y., A. Hasegawa, A. Takamori, A. Sasada, R. Tanosaki, I. Choi, A. Utsunomiya, Y. Maeda, Y. Yamano, T. Eto, et al. 2013. Potential contribution of a novel Tax epitope-specific CD4+ T cells to graft-versus-Tax effect in adult T cell leukemia patients after allogeneic hematopoietic stem cell transplantation. *J. Immunol.* 190: 4382–4392.
12. Nishikawa, H., Y. Maeda, T. Ishida, S. Gnjatic, E. Sato, F. Mori, D. Sugiyama, A. Ito, Y. Fukumori, A. Utsunomiya, et al. 2012. Cancer/testis antigens are novel targets of immunotherapy for adult T-cell leukemia/lymphoma. *Blood* 119: 3097–3104.
13. Itonaga, H., H. Tsushima, J. Taguchi, T. Fukushima, H. Taniguchi, S. Sato, K. Ando, Y. Sawayama, E. Matsuo, R. Yamasaki, et al. 2013. Treatment of relapsed adult T-cell leukemia/lymphoma after allogeneic hematopoietic stem cell transplantation: the Nagasaki Transplant Group experience. *Blood* 121: 219–225.
14. Ishida, T., M. Hishizawa, K. Kato, R. Tanosaki, T. Fukuda, Y. Takatsuka, T. Eto, Y. Miyazaki, M. Hidaka, N. Uike, et al. 2013. Impact of Graft-versus-Host Disease on Allogeneic Hematopoietic Cell Transplantation for Adult T Cell Leukemia-Lymphoma Focusing on Preconditioning Regimens: Nationwide Retrospective Study. *Biol. Blood Marrow Transplant.* 19: 1731–1739.
15. Poiesz, B. J., F. W. Ruscetti, A. F. Gazdar, P. A. Bunn, J. D. Minna, and R. C. Gallo. 1980. Detection and isolation of type C retrovirus particles from fresh and cultured lymphocytes of a patient with cutaneous T-cell lymphoma. *Proc. Natl. Acad. Sci. USA* 77: 7415–7419.
16. Hinuma, Y., K. Nagata, M. Hanaoka, M. Nakai, T. Matsumoto, K. I. Kinoshita, S. Shirakawa, and I. Miyoshi. 1981. Adult T-cell leukemia: antigen in an ATL cell line and detection of antibodies to the antigen in human sera. *Proc. Natl. Acad. Sci. USA* 78: 6476–6480.
17. Gonçalves, D. U., F. A. Proietti, J. G. Ribas, M. G. Araújo, S. R. Pinheiro, A. C. Guedes, and A. B. Carneiro-Proietti. 2010. Epidemiology, treatment, and prevention of human T-cell leukemia virus type 1-associated diseases. *Clin. Microbiol. Rev.* 23: 577–589.
18. Grassmann, R., C. Dengler, I. Müller-Fleckenstein, B. Fleckenstein, K. McGuire, M. C. Dokhelar, J. G. Sodroski, and W. A. Haseltine. 1989. Transformation to continuous growth of primary human T lymphocytes by human T-cell leukemia virus type I X-region genes transduced by a Herpesvirus saimiri vector. *Proc. Natl. Acad. Sci. USA* 86: 3351–3355.
19. Tanaka, A., C. Takahashi, S. Yamaoka, T. Nosaka, M. Maki, and M. Hatanaka. 1990. Oncogenic transformation by the tax gene of human T-cell leukemia virus type I in vitro. *Proc. Natl. Acad. Sci. USA* 87: 1071–1075.
20. Akagi, T., and K. Shimotohno. 1993. Proliferative response of Tax1-transduced primary human T cells to anti-CD3 antibody stimulation by an interleukin-2-independent pathway. *J. Virol.* 67: 1211–1217.
21. Hinrichs, S. H., M. Nerenberg, R. K. Reynolds, G. Khoury, and G. Jay. 1987. A transgenic mouse model for human neurofibromatosis. *Science* 237: 1340–1343.
22. Nerenberg, M., S. H. Hinrichs, R. K. Reynolds, G. Khoury, and G. Jay. 1987. The tat gene of human T-lymphotropic virus type 1 induces mesenchymal tumors in transgenic mice. *Science* 237: 1324–1329.
23. Hasegawa, H., H. Sawa, M. J. Lewis, Y. Orba, N. Sheehy, Y. Yamamoto, T. Ichinohe, Y. Tsunetsugu-Yokota, H. Katano, H. Takahashi, et al. 2006. Thymus-derived leukemia-lymphoma in mice transgenic for the Tax gene of human T-lymphotropic virus type I. *Nat. Med.* 12: 466–472.
24. Ohsugi, T., T. Kumasaka, S. Okada, and T. Urano. 2007. The Tax protein of HTLV-1 promotes oncogenesis in not only immature T cells but also mature T cells. *Nat. Med.* 13: 527–528.
25. Satou, Y., J. Yasunaga, M. Yoshida, and M. Matsuoka. 2006. HTLV-I basic leucine zipper factor gene mRNA supports proliferation of adult T cell leukemia cells. *Proc. Natl. Acad. Sci. USA* 103: 720–725.
26. Satou, Y., J. Yasunaga, T. Zhao, M. Yoshida, P. Miyazato, K. Takai, K. Shimizu, K. Ohshima, P. L. Green, N. Ohkura, et al. 2011. HTLV-1 bZIP factor induces T-cell lymphoma and systemic inflammation in vivo. *PLoS Pathog.* 7: e1001274.
27. Fan, J., G. Ma, K. Nosaka, J. Tanabe, Y. Satou, A. Koito, S. Wain-Hobson, J. P. Vartanian, and M. Matsuoka. 2010. APOBEC3G generates nonsense mutations in human T-cell leukemia virus type 1 proviral genomes in vivo. *J. Virol.* 84: 7278–7287.
28. Takeda, S., M. Maeda, S. Morikawa, Y. Taniguchi, J. Yasunaga, K. Nosaka, Y. Tanaka, and M. Matsuoka. 2004. Genetic and epigenetic inactivation of tax gene in adult T-cell leukemia cells. *Int. J. Cancer* 109: 559–567.
29. Suemori, K., H. Fujiwara, T. Ochi, T. Ogawa, M. Matsuoka, T. Matsumoto, J. M. Mesnard, and M. Yasukawa. 2009. HBZ is an immunogenic protein, but not a target antigen for human T-cell leukemia virus type 1-specific cytotoxic T lymphocytes. *J. Gen. Virol.* 90: 1806–1811.
30. Macnamara, A., A. Rowan, S. Hilburn, U. Kadolsky, H. Fujiwara, K. Suemori, M. Yasukawa, G. Taylor, C. R. Bangham, and B. Asquith. 2010. HLA class I binding of HBZ determines outcome in HTLV-1 infection. *PLoS Pathog.* 6: e1001117.
31. Enose-Akahata, Y., A. Abrams, R. Massoud, I. Bialuk, K. R. Johnson, P. L. Green, E. M. Maloney, and S. Jacobson. 2013. Humoral immune response to HTLV-1 basic leucine zipper factor (HBZ) in HTLV-1-infected individuals. *Retrovirology* 10: 19.
32. Shimoyama, M. 1991. Diagnostic criteria and classification of clinical subtypes of adult T-cell leukaemia-lymphoma. A report from the Lymphoma Study Group (1984-87). *Br. J. Haematol.* 79: 428–437.
33. Ishida, T., A. Utsunomiya, S. Iida, H. Inagaki, Y. Takatsuka, S. Kusumoto, G. Takeuchi, S. Shimizu, M. Ito, H. Komatsu, et al. 2003. Clinical significance of CCR4 expression in adult T-cell leukemia/lymphoma: its close association with skin involvement and unfavorable outcome. *Clin. Cancer Res.* 9: 3625–3634.
34. MacNamara, A., U. Kadolsky, C. R. Bangham, and B. Asquith. 2009. T-cell epitope prediction: rescaling can mask biological variation between MHC molecules. *PLOS Comput. Biol.* 5: e1000327.
35. Rende, F., I. Cavallari, A. Corradin, M. Silic-Benussi, F. Toulza, G. M. Toffolo, Y. Tanaka, S. Jacobson, G. P. Taylor, D. M. D'Agostino, et al. 2011. Kinetics and intracellular compartmentalization of HTLV-1 gene expression: nuclear retention of HBZ mRNAs. *Blood* 117: 4855–4859.
36. Hilburn, S., A. Rowan, M. A. Demontis, A. MacNamara, B. Asquith, C. R. Bangham, and G. P. Taylor. 2011. In vivo expression of human T-lymphotropic virus type 1 basic leucine-zipper protein generates specific CD8+ and CD4+ T-lymphocyte responses that correlate with clinical outcome. *J. Infect. Dis.* 203: 529–536.
37. Yamano, Y., and T. Sato. 2012. Clinical pathophysiology of human T-lymphotropic virus-type 1-associated myelopathy/tropical spastic paraparesis. *Front. Microbiol.* 3: 389.

Journal of Dermatological Science 73 (2014) 209–215

Contents lists available at ScienceDirect

Journal of Dermatological Science

journal homepage: www.jdsjournal.com

TLR4 and NLRP3 inflammasome activation in monocytes by *N*-propionyl cysteaminylphenol-maleimide-dextran (NPCMD)

Yu Mizote [a,b], Kazumasa Wakamatsu [c], Shosuke Ito [c], Akiko Uenaka [d], Yoshihiro Ohue [b], Koji Kurose [b], Midori Isobe [b], Akira Ito [e], Yasuaki Tamura [f], Hiroyuki Honda [g], Toshiharu Yamashita [h], Satoshi Nohara [i], Mikio Oka [b], Kowichi Jimbow [h], Eiichi Nakayama [d,*]

[a] *Department of Immunology, Okayama University Graduate School of Medicine, Dentistry and Pharmaceutical Sciences, Okayama, Japan*
[b] *Department of Respiratory Medicine, Kawasaki Medical School, Kurashiki, Japan*
[c] *Department of Chemistry, Fujita Health University School of Health Sciences, Toyoake, Japan*
[d] *Faculty of Health and Welfare, Kawasaki University of Medical Welfare, Kurashiki, Japan*
[e] *Department of Chemical Engineering, Faculty of Engineering, Kyusyu University, Fukuoka, Japan*
[f] *Department of Pathology, Sapporo Medical Univeristy School of Medicine, Sapporo, Japan*
[g] *Department of Biotechnology, School of Engineering, Nagoya University, Nagoya, Japan*
[h] *Department of Dermatology, Sapporo Medical Univeristy School of Medicine, Sapporo, Japan*
[i] *Meito Sangyo Co., Nagoya, Japan*

ARTICLE INFO

Article history:
Received 6 September 2013
Received in revised form 7 November 2013
Accepted 7 November 2013

Keywords:
Toll-like receptors (TLR)
Nod-like receptors (NLR)
Tyrosinase
Melanogenesis

ABSTRACT

Background: *N*-propionyl cysteaminylphenol-maleimide-dextran (NPCMD) is a toxic tyrosinase substrate developed to treat melanoma.
Objective: We investigated the effect of NPCMD on innate immune responses in monocytes.
Methods: $CD14^+$ monocytes and a monocytic cell line, THP-1, were stimulated with NPCMD in vitro. Cytokines in the culture supernatants were determined by ELISA and flow cytometry.
Results: NPCMD stimulated $CD14^+$ monocytes and THP-1 cells to secrete TNFα, IL-6 and IL-8, but not IL-10 or IL-12. TNFα secretion from THP-1 cells stimulated with NPCMD was inhibited by addition of an anti-TLR4 mAb in culture. Moreover, NPCMD stimulated production of pro-IL-1β in $CD14^+$ monocytes and monocytic cell line THP-1 cells and activated the NLRP3-inflammasome, resulting in production of mature IL-1β. Use of ASC and NLRP3-deficient THP-1 cell lines established involvement of the NLRP3 inflammasome in an IL-1β secretion in treatment with NPCMD. Inhibition of IL-1β secretion by an endocytosis inhibitor, cytochalasin B, and a lysosomal enzyme cathepsin B inhibitor, CA-074 Me, suggested the involvement of lysosomal rupture and leakage of cathepsin B into the cytosol in NLRP3 activation by NPCMD.
Conclusion: The immunopotentiating effect of NPCMD mediated by TLR4 and NLRP3 inflammasome activation could be useful for eliciting effective adaptive immune responses against melanoma and other tumors.

1. Introduction

Melanogenesis is a biosynthetic pathway in the cytosolic organelle melanosome in a melanocyte and a melanoma cell. The enzyme tyrosinase catalyzes oxidative conversion of L-tyrosine via dopaquinone to a melanin pigment [1,2]. Therapeutic agents specific to melanoma have been studied in terms of utilizing this unique biosynthetic pathway. Monobenzone (hydroquinone monobenzyl ether) is a strong inducer of skin depigmentation (vitiligo) and also causes application-related dermatitis [3–5]. Its depigmenting action depends on its conversion by tyrosinase and the subsequent formation of benzoquinone, which binds to cysteine residues in

Abbreviations: 4-*S*-CAP, 4-*S*-cysteaminylphenol; alum, aluminum hydroxide; APDC, (2R,4R)-4-aminopyrrolidine-2, 4-dicarboxylic acid; ATP, adenosine triphosphate; CBA, cytometric bead array; CMD, carboxymethyl dextran; DAMP, danger-associated molecular pattern; defASC, ASC-deficient THP-1; defNLRP3, NLRP3-deficient THP-1; FBS, fetal bovine serum; LAL, limulus amebocyte lysate; LPS, lipopolysaccharide; MIL, maleimide linker; MIL-CMD, maleimide linker conjugated carboxymethyl dextran; MTT, methylthiazole tetrazolium; NPCMD, *N*-propionyl-4-*S*-cysteaminylphenol-maleimide-dextran; NPrCAP, *N*-propionyl-4-*S*-cysteaminyl-phenol; PAMP, pathogen-associated molecular pattern; PBMCs, peripheral blood mononuclear cells; RQ, relative quantification.

* *Corresponding author at*: Faculty of Health and Welfare, Kawasaki University of Medical Welfare, 288 Matsushima, Kurashiki, Okayama 701-0193, Japan. Tel.: +81 86 462 1111x54954; fax: +81 86 464 1109.
E-mail address: nakayama@mw.kawasaki-m.ac.jp (E. Nakayama).

0923-1811/$36.00 © 2013 Japanese Society for Investigative Dermatology. Published by Elsevier Ireland Ltd. All rights reserved.
http://dx.doi.org/10.1016/j.jdermsci.2013.11.006

melanosome and other proteins. Subsequently, the haptenated proteins sensitize skin [6]. It is strongly cytotoxic to melanoma cells, which probably uptake monobenzone specifically compared to other cell types [7]. Its cytotoxicity is independent of the presence of the tyrosinase enzyme [6,7] and therefore it is not in use systemically. Jimbow and his colleagues have developed less toxic and feasible therapeutic chemicals for melanoma using tyrosine analogs [8]. A sulfur-amine analog of tyrosine, 4-*S*-cysteaminylphenol (4-*S*-CAP), was produced and an *N*-protected analog of 4-*S*-CAP, *N*-propionyl-4-*S*-cysteaminylphenol (NPrCAP), was stable for degradation [9]. Furthermore, recently, to increase the solubility of NPrCAP, carboxymethyl dextran (CMD) was conjugated to it using a maleimide linker (MIL). Thus, NPrCAP-CMD (NPCMD) was expected to diffuse efficiently in tumor tissue. These phenols have been shown to be good substrates for tyrosinase [9], are selectively incorporated into melanoma cells and showed cytotoxicity in vitro and in vivo [9–11]. Moreover, adaptive immunity elicited against melanoma was shown to be involved in an NPrCAP-mediated anti-melanoma effect [12].

Inflammasomes are cytosolic sensors that rapidly activate the caspase-1 protease in response to various pathogen-associated molecular patterns (PAMPs) or host-derived signals of cellular stress (danger-associated molecular patterns, DAMPs) [13]. Caspase-1 cleaves and activates two pro-inflammatory cytokines, IL-1β and IL-18. Memory T-cell responses play an important role in adaptive immunity. There is some evidence of innate activation of memory T-cell responses without involving T-cell antigen receptor signaling [14,15]. Recently, it was shown that memory CD8 T-cells in some bacterial infections were activated by IL-18 released following NLRC4 inflammasome activation in the absence of T-cell antigen receptor activation [16]. In this study, we investigated the activation of innate immune responses by NPCMD instead of its direct effect on melanoma. We show that NPCMD stimulated $CD14^+$ monocytes and monocytic cell line THP-1 cells to secrete TNFα via TLR4, and IL-1β by NLRP3 activation. Efficient activation of innate immunity by NPCMD could facilitate adaptive immunity against melanoma and other tumors.

2. Materials and methods

2.1. Reagents

All chemicals were of the highest purity available. 3-Mercaptopropionic acid, *N,N'*-dicyclohexylcarbodiimide, 1-hydroxybenzotriazole, *N,N*-dimethylformamide, and *N*-hydroxysuccinimide were purchased from Tokyo Chemical Industry Co., LTD. (Tokyo, Japan). 1-Ethyl-3-(3-dimethylaminopropyl) carbodiimide hydrochloride was purchased from Dojindo Laboratories (Kumamoto, Japan). Carboxymethyl dextran (M.W. 10,000) and *N*-(2-aminoethyl) maleimide hydrochloride were synthesized at Meito Sangyo Co. (Nagoya, Japan). 4-*S*-CAP and NPrCAP were prepared by the method of Padgette et al. [17] and Tandon et al. [9], respectively. Adenosine triphosphate (ATP), cytochalasin B, dextranase, lipopolysaccharide (LPS), methylthiazole tetrazolium (MTT) and polymyxin B were purchased from Sigma–Aldrich (St. Louis, MO). The caspase-1 inhibitor z-YVAD-fmk and (2R, 4R)-4-aminopyrrolidine-2, 4-dicarboxylic acid (APDC) were from Enzo Life Sciences (Farmingdale, NY). CA-074 Me was from Merck Millipore (Billerica, MA). A double strand DNA analog poly (dA:dT) was from InvivoGen (San Diego, CA). Aluminum hydroxide (alum) was from Katayama Chemical (Osaka, Japan).

2.2. Synthesis of N-propionyl cysteaminylphenol-maleimide-dextran (NPCMD)

1.4 g (12.2 mmol) *N*-hydroxysuccinimide and 2.3 g (12.0 mmol) 1-ethyl-3-(3-dimethylaminopropyl) carbodiimide hydrochloride were added to 5.4 g (0.54 mmol) carboxymethyldextran in 52 mL water, and were stirred for 1 h at room temperature. 1.56 g (8.83 mmol) *N*-(2-aminoethyl) maleimide hydrochloride in 52 mL of 0.2 mol/L boric buffer (pH 8.5) was stirred in a reactor adding the above reaction mixture. After 18 h at room temperature, the reaction mixture was washed by flowing water through the dialysis membrane (M.W. 1000) overnight. The solution was dried to a powder under freeze-drying conditions to give 5.33 g of maleimide linker conjugated carboxymethyl dextran (MIL-CMD) (99%). 2.6 g MIL-CMD in 200 mL water was added slowly to 0.33 g NPrCAP-SH in 35 mL THF and stirred for 1 h at room temperature. The reaction mixture was evaporated to remove THF and filtrated. The filtrate was washed by flowing water through the dialysis membrane (M.W. 1000) overnight. The resulting solution was dried to a powder under freeze-drying conditions to give 2.37 g NPCMD (91%).

2.3. Blood samples

Peripheral blood was drawn from healthy donors after obtaining written informed consent. Peripheral blood mononuclear cells (PBMCs) were isolated by density gradient centrifugation using Histopaque 1077 (Sigma–Aldrich). $CD3^+$, $CD14^+$, $CD19^+$ and $CD56^+$ cells were purified from PBMCs using CD3, CD14, CD19 and CD56 microbeads, respectively, using an autoMACS (Miltenyi Biotec, Auburn, CA). The residual cells were used as $Lineage^-$ cells.

2.4. Cell lines

THP-1, an acute monocytic leukemia cell line was obtained from ATCC. NLRP3-deficient THP-1 (defNLRP3) and ASC-deficient THP-1 (defASC) were obtained from InvivoGen. The medium used to maintain these cell lines was RPMI 1640 supplemented with 10% fetal bovine serum (FBS) (JRM Bioscience, Lenexa, KA).

2.5. Quantitative real-time RT-PCR

Total RNA was obtained from cells using an RNeasy Mini kit (Qiagen, Chatsworth, CA) according to the manufacturer's instructions. 500 nanograms of each sample were subjected to cDNA synthesis using a PrimeScript RT Master Mix (Takara Bio, Shiga, Japan). Two-step real-time RT-PCR was run on an Mx3000P QPCR System (Agilent Technologies, Santa Clara, CA). The primers were: *ASC* 5′-TGGTCAGCTTCTACCTGGAGACCTA-3′ (forward), 5′-CTTGGCTGCCGACTGAGGAG-3′ (reverse), *IL-1β* 5′-ACAGATGAAGTGCTCCTTCCA-3′ (forward), 5′-GTCGGAGATTCGTAGCTGGAT-3′ (reverse), *NLRP3* 5′-CTGCGATCAACAGGAGAGACCTTT-3′ (forward), 5′-ACCCATCCACTCCTCTTCAATGCT-3′ (reverse), *GAPDH* 5′-GCTCTCTGCTCCTCCTGTTC-3′ (forward), 5′-ACGACCAAATCCGTTGACTC-3′ (reverse). The TaqMan probes were: *ASC* 5′-FAM-TCACCGCTAACGTGCTGCGCGACAT-TAMRA-3′, *IL-1β* 5′-FAM-CTCT GCCCTCTGGATGGCGG-TAMRA-3′, *NLRP3* 5′-FAM-TGCACGTGTTTC-GAATCCCACTGTGA-TAMRA-3′, *GAPDH* 5′-HEX-AGCCACATCGCTCA-GACACCATGGG-BHQ1-3′. PCR was performed with FastStart Universal Probe Master (ROX) (Roche Applied Science, Upper Bavaria, Germany), the primer pair, the TaqMan probe, and cDNA solution. The thermal cycling conditions comprised an initial denaturation step at 95 °C for 10 min, followed by 45 cycles of 95 °C for 15 s and 60 °C for 1 min. The mRNA expression level of each target gene was normalized to the expression level of GAPDH.

2.6. MTT assay

$CD3^+$, $CD14^+$, $CD19^+$, $CD56^+$, $Lineage^-$ and THP-1 cells (1×10^5) were cultured in a 96-well round culture plate in 10% FBS-RPMI 1640 medium with NPCMD for 1 day at 37 °C. After incubation, the medium was removed and serum-free RPMI1640 medium

containing MTT (0.5 mg/mL) was added. After an additional incubation for 3 h at 37 °C, the medium was removed and DMSO was added to each well. The absorbance was read at 535 nm.

2.7. Endotoxin detection

Endotoxin was estimated using Limulus Amebocyte Lysate (LAL) Kinetic-QCL (Lonza, Allendale, NJ) according to the manufacturer's instructions.

2.8. ELISA to detect dextran

NPCMD (1 μg/mL) with various amounts of polymyxin B or dextranase in a coating buffer were adsorbed onto a 96-well ELISA plate (Nunc, Roskilde, Denmark) and incubated overnight at 4 °C. After washing and blocking, mouse anti-dextran mAb (STEMCELL Technologies, Vancouver, Canada) was added and incubation was done for 2 h at 37 °C. After washing, a horseradish peroxidase (HRP)-conjugated goat anti-mouse IgG (MBL, Nagoya, Japan) was added and incubation was done for 1 h at 37 °C. After washing and development, absorbance was read at 490 nm.

2.9. Cytokine detection

Supernatants from cultures of $CD3^+$, $CD14^+$, $CD19^+$, $CD56^+$, $Lineage^-$ and THP-1 cells (1×10^5) treated with NPCMD were collected and the amounts of IL-1β, IL-6, IL-8, IL-10, IL-12p70 and TNFα were estimated using a Cytometric Bead Array (CBA) kit (BD Biosciences, San Jose, CA) by FACS Canto II.

2.10. IL-1β and TNFα ELISA

THP-1 cells (1×10^5) were treated with the indicated amounts of NPCMD, NPrCAP, MIL-CMD, alum, ATP or poly (dA:dT) in the presence or absence of LPS. The cytokines in the culture supernatants or cell lysates were estimated by DuoSet Sandwich ELISAs (R&D Systems, Minneapolis, MN), according to the manufacturer's instructions. For the inhibition assay, the indicated amounts of anti-TLR4 mAb (Santa Cruz Biotechnology, Santa Cruz, CA), polymyxin B, z-YVAD-fmk, cytochalasin B, CA-074 Me and APDC were added to the assay culture.

2.11. Statistical analysis

The values are expressed as the mean ± S.D. of individual samples. The significance of the results was determined using the Student's *t* test. *P* values less than 0.05 were considered statistically significant.

3. Results

3.1. Endotoxin-like activity of NPCMD

As shown in Fig. 1A, to increase the solubility of NPrCAP and make it diffuse efficiently in tissue, CMD was conjugated using the MIL. First, we examined the endotoxin-like activity of NPrCAP and its CMD conjugate (NPCMD) with an LAL test. As shown in Fig. 1B, moderate endotoxin-like activity was detected in NPCMD, but not its components, NPrCAP or MIL-CMD alone at an equivalent amount included in NPCMD. To examine the possibility that the endotoxin-like activity observed in the NPCMD preparation was indeed due to LPS contaminating the preparation, we examined the effect of polymyxin B treatment of NPCMD in an endotoxin assay. As shown in Fig. 1C, while the endotoxin activity of LPS was diminished completely, the endotoxin-like activity of NPCMD was not diminished by the treatment. On the other hand, while no reduction in endotoxin activity of LPS was observed by dextranase treatment, the endotoxin-like activity of NPCMD was reduced by

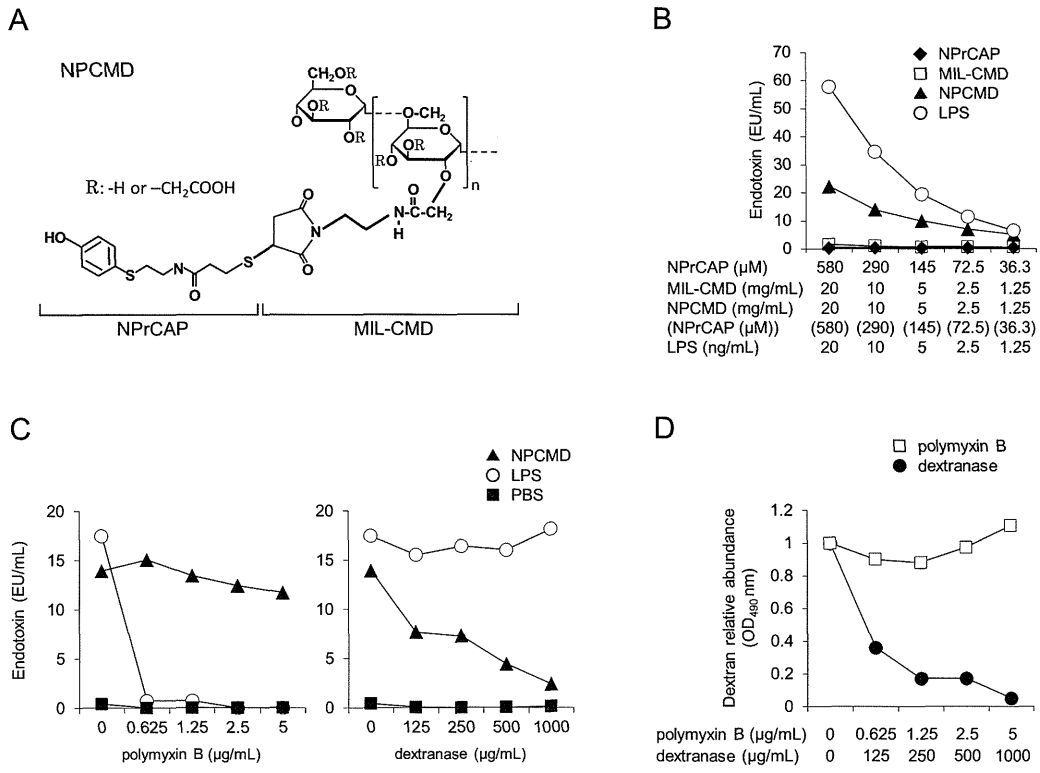

Fig. 1. Endotoxin assay of NPCMD. (A) Structural formula of NPCMD. (B) and (C) LAL test for endotoxin. (D) ELISA for dextran in NPCMD (1 μg/mL) using an anti-dextran mAb. In (C) and (D), NPCMD (10 mg/mL), LPS (5 ng/mL) and PBS (control) were pre-treated with polymyxin B or dextranase. These results are representative from three independent experiments.

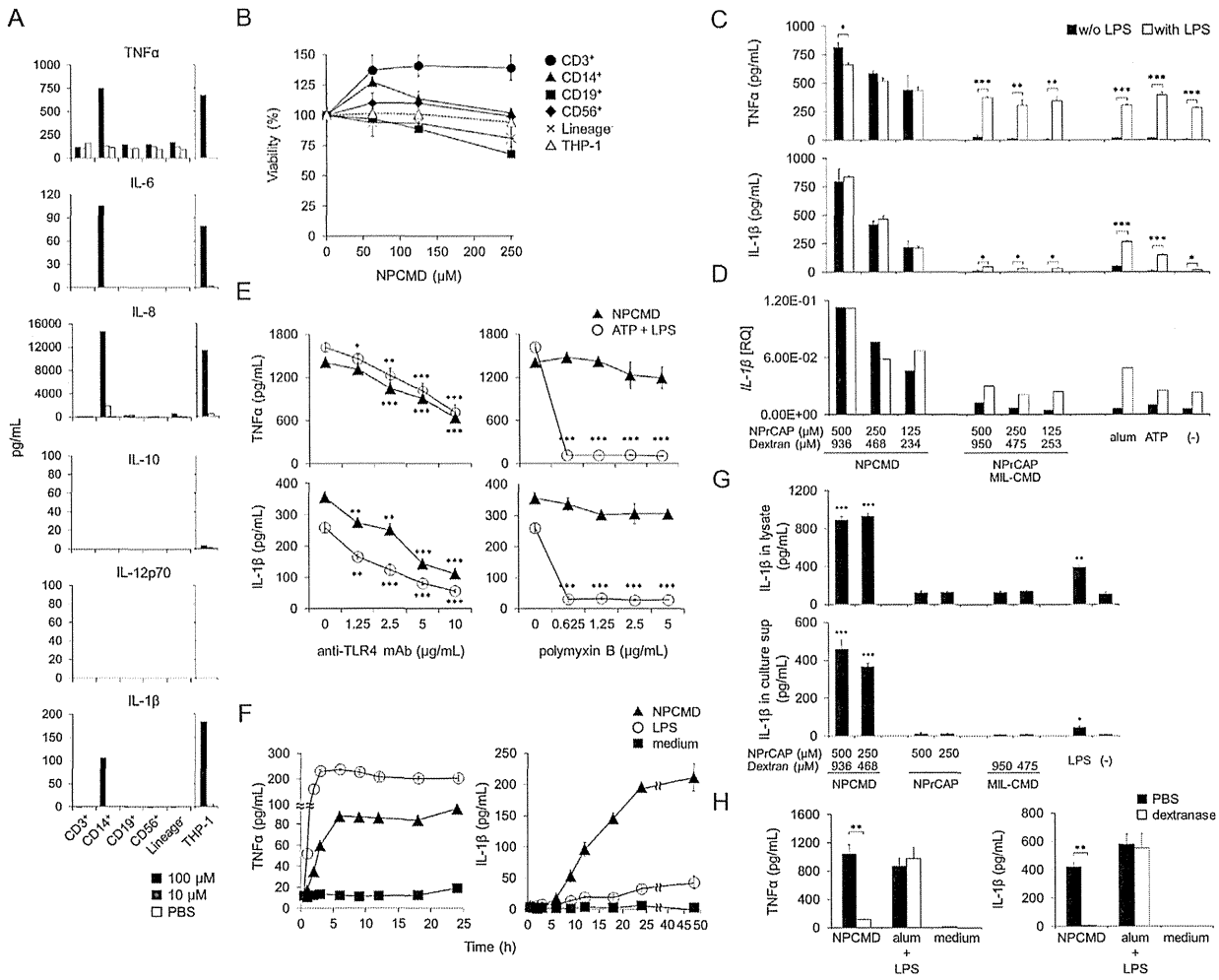

Fig. 2. Cytokine release from CD14$^+$ monocytes and THP-1 cells after treatment with NPCMD. (A) CD3$^+$, CD14$^+$, CD19$^+$, CD56$^+$, Lineage$^-$ and THP-1 cells (1×10^5) were treated with NPCMD (containing 100 or 10 μM NPrCAP) for 48 h. Cytokines in the culture supernatants were determined with a CBA kit. The assays were done in duplicate and the values represent the mean. (B) CD3$^+$, CD14$^+$, CD19$^+$, CD56$^+$, Lineage$^-$ or THP-1 cells (1×10^5) were treated with NPCMD at the indicated concentrations. Viability of cells was measured after 24 h by MTT assay. The viability (percentage) was calculated relative to untreated (control) cells. The assays were done in triplicate and the values represent the mean ± S.D. (C) and (D) THP-1 cells (1×10^5) were treated with NPCMD, NPrCAP plus MIL-CMD, alum (25 μg/mL) or ATP (1 μM) with or without (w/o) LPS (100 pg/mL) for 18 h. In (D), the mRNA level of IL-1β was quantified by real-time RT-PCR. RQ, relative quantification. In (C), the assays were done in triplicate and the values represent the mean ± S.D. In (D), the assays were done in duplicate and the values represent the mean. (E) THP-1 cells (1×10^5) were treated with NPCMD (containing 200 μM NPrCAP) or ATP (1 μM) plus LPS (50 pg/mL) in the presence of the indicated amounts of anti-TLR4 mAb or polymyxin B for 18 h. The assays were done in triplicate and the values represent the mean ± S.D. (F) THP-1 cells (5×10^4) were treated with NPCMD (containing 200 μM NPrCAP) or LPS (1 ng/mL) for the indicated times. The assays were done in triplicate and the values represent the mean ± S.D. (G) THP-1 cells (1×10^5) were treated with NPCMD, NPrCAP, MIL-CMD or LPS (1 ng/mL) for 12 h. After treatment, the cells were lysed by cycles of freeze-thawing. The assays were done in triplicate and the values represent the mean ± S.D. (H) THP-1 cells (1×10^5) were treated with NPCMD (containing 200 μM NPrCAP) or alum (25 μg/mL) plus LPS (50 pg/mL) for 18 h after no treatment or pre-treatment with dextranase (0.5 mg/mL). TNFα and IL-1β in the supernatant in (C), (E), (F), (G) and (H), and pro-IL-1β and mature IL-1β in the cell lysate in (G) were determined by ELISA. Statistical analyses were performed with the Student's *t* test; $^*P < 0.05$, $^{**}P < 0.01$, $^{***}P < 0.001$.

the same treatment. Dextran degradation by dextranase treatment determined by ELISA using an anti-dextran mAb (Fig. 1D) was consistent with the reduction in endotoxin-like activity in NPCMD in Fig. 1C.

Collectively, the findings show that the conjugated product NPCMD had moderate endotoxin-like activity in the LAL test, while its components NPrCAP and MIL-CMD showed no such activity. The endotoxin-like activity of NPCMD was dependent on dextran in the molecule.

3.2. Cytokine release from CD14$^+$ monocytes and the monocytic cell line THP-1 following treatment with NPCMD

CD3$^+$, CD14$^+$, CD19$^+$ and CD56$^+$ cells were purified using magnetic beads coated with the respective antibody and treated with NPCMD. As shown in Fig. 2A, only CD14$^+$ cells were reactive to NPCMD and secreted TNFα, IL-6, IL-8 and IL-1β, but not IL-10 or IL-12p70. Essentially similar results were obtained with the monocytic cell line THP-1. While NPCMD was toxic to melanoma as NPrCAP [11,12,18,19], no cytotoxicity was observed with PBMCs and THP-1 cells following treatment with NPCMD in an MTT assay (Fig. 2B). We investigated secretion of TNFα and IL-1β from THP-1 cells treated with NPCMD, and its components NPrCAP or MIL-CMD at an equivalent amount included in NPCMD. As shown in Fig. 2C, those cytokine secretions were observed only by treatment with NPCMD, but not its component NPrCAP or MIL-CMD alone or their mixture. The effect of LPS on TNFα or IL-1β secretion from THP-1 cells treated with NPCMD was then investigated. No augmentation of cytokine secretion by addition of LPS was observed (Fig. 2C). Quantitative real-time RT-PCR analysis showed a dose-dependent elevation of *IL-1β* mRNA levels in THP-1 cells treated with NPCMD (Fig. 2D). We then examined whether the secretion of TNFα and IL-1β was due to activation of the TLR4 pathway by antibody blocking using an anti-TLR4 mAb. As shown in Fig. 2E, the secretion of TNFα and IL-1β was blocked by addition of an anti-TLR4 mAb to the culture. These findings suggested that

NPCMD stimulated monocytes and THP-1 cells through the TLR4 pathway and secreted TNFα and IL-1β. Moreover, TNFα or IL-1β production from THP-1 cells by LPS plus ATP, but not by NPCMD, was diminished by treatment with polymyxin B, suggesting no involvement of LPS in those cytokine secretions in NPCMD stimulation. As shown in Fig. 2F, secretion of TNFα occurred as early as 2 h after NPCMD treatment, being comparable to LPS, while IL-1β secretion was only observed 6 h after treatment, indicating secretion of IL-1β following TNFα. IL-1β secretion was shown to occur by caspase-1 mediated degradation of pro-IL-1β to its mature form. Activation of caspase-1 occurs by activation of a multi-protein complex known as inflammasome. Pro-caspase-1 formed a multiplex by binding to the effector site of inflammasome, autocatalizing the molecule to active caspase-1 and cleaving pro-IL-1β to produce its active form. Therefore, production of pro-IL-1β was necessary before inflammasome activation to produce IL-1β. The results in Fig. 2G suggested that pro-IL-1β was produced in the cytosol of THP-1 in the treatment with NPCMD and IL-1β was secreted in the culture supernatant. Furthermore, as shown in Fig. 2H, TNFα and IL-1β secretion from THP-1 cells by NPCMD was diminished by dextranase treatment, indicating its dextran-dependent activation consistent with the results shown in Fig. 1. Endotoxin-like activity of NPCMD through the TLR4 pathway likely primed monocytes and THP-1 cells to produce pro-IL-1β in the cytosol, and thereafter secrete IL-1β efficiently with the same NPCMD stimulation.

3.3. Involvement of NLRP3 inflammasome activation for IL-1β secretion from THP-1 cells treated with NPCMD

The effect of z-YVAD-fmk, a peptide inhibitor of active caspase-1 on IL-1β secretion from THP-1 cells treated with NPCMD was examined. As shown in Fig. 3A, dose-dependent inhibition of IL-1β secretion, but not TNFα secretion, was observed. A similar effect was observed in IL-1β secretion from THP-1 cells treated with alum plus LPS or ATP plus LPS, both of which were shown to stimulate NLRP3 inflammasome activation to produce IL-1β in THP-1 cells [20,21].

To investigate whether NLRP3 inflammasome activation was involved in IL-1β secretion from THP-1 cells treated with NPCMD, we utilized ASC- and NLRP3-deficient THP-1 cell lines. As shown in Fig. 3B, no *ASC* or *NLRP3* mRNA expression was observed in ASC-deficient or NLRP3-deficient THP-1 cells, respectively. As shown in Fig. 3C, while TNFα secretion from either ASC or NLRP3 deficient THP-1 cells was observed by treatment with NPCMD, as well as alum plus LPS or ATP plus LPS, no IL-1β secretion was observed from either cell type. However, IL-1β secretion was observed in NLRP3-deficient, but not ASC-deficient THP-1 cells, treated with a double stranded DNA analog poly (dA:dT), which is a ligand of the AIM2 inflammasome plus LPS [22]. These findings suggested that NPCMD stimulated TNFα as well as IL-6 and IL-8 secretion from THP-1 cells through TLR4 signaling and IL-1β secretion through NLRP3 inflammasome activation. To secrete IL-1β, accumulation of pro-IL-1β is necessary [23]. The results suggested that pro-IL-1β was preformed through TLR4 signaling by NF-κB activation and cleaved it to mature IL-1β by active caspase-1 produced by autocleavage of pro-caspase-1 following NLRP3 inflammasome activation by NPCMD.

NLRP3 inflammasome activation was shown to occur following endocytosis of bacterial PAMPs and endogenous danger signals like DAMPs, resulting in lysosomal rupture. Therefore, we examined the effect of the endocytosis inhibitor cytochalasin B and the lysosomal enzyme cathepsin B inhibitor CA-074 Me as shown in Figs. 3D and E, respectively. Cytochalasin B inhibited IL-1β secretion from THP-1 cells treated with NPCMD or alum plus LPS, but not ATP plus LPS. CA-074 Me inhibited IL-1β secretion from THP-1 cells treated with NPCMD, as well as alum plus LPS or ATP plus LPS. Furthermore, ROS have been shown to cause NLRP3 inflammasome activation [13,24]. The ROS inhibitor APDC, however, showed only marginal inhibition of IL-1β secretion from THP-1 cells treated with NPCMD or ATP plus LPS. No inhibition was observed with alum plus LPS treatment.

4. Discussion

In this study, we showed that NPCMD, but not its components NPrCAP or MIL-CMD alone or their mixture, gives rise to a positive reaction in a standard LAL test used to detect endotoxin in a dextran-dependent manner that was included in the molecule. These findings suggested that the positive reaction of NPCMD in the LAL test was likely due to the conformation derived from combining NPrCAP and MIL-CMD. In this regard, dextran contains α-1, 6 glycoside glucose predominantly. In the LAL test, β-glucan (β1-3 glucose) from fungus is known to give a positive reaction [25]. Although the positivity of NPCMD in the LAL test may not be directly linked to its endototoxin-like activity, NPCMD indeed showed endotoxin-like activity. NPCMD stimulated $CD14^+$ monocytes and monocytic cell line THP-1 cells to secrete TNFα, IL-6 and IL-8, but not IL-10 or IL-12 by itself. Moreover, TNFα secretion from THP-1 cells was inhibited by the addition of an anti-TLR4 mAb in culture. Production of IL-1β and IL-18 was mediated by inflammasome activation, which resulted in autocleavage of pro-caspase-1 bound to inflammasome by its proximity in multiplex formation to active caspase-1. Pro-IL-1β and pro-IL-18 preformed in the cytosol were cleaved to proinflammatory cytokine IL-1β and IL-18, respectively, by caspase-1. NPCMD stimulated production of pro-IL-1β and pro-IL-18 (data not shown) via NF-κB activation (data not shown) in monocytic cell line THP-1 cells, and activated the NLRP3 inflammasome resulting in production of mature IL-1β and IL-18. Use of ASC and NLRP3-deficient THP-1 cell lines established the involvement of NLRP3 inflammasome in IL-1β and IL-18 secretion in stimulation with NPCMD. While TNFα was secreted from either ASC-deficient or NLRP3-deficient THP-1 cells in stimulation with NPCMD, no IL-1β secretion was observed. A double stranded DNA analog, poly (dA:dT), which is the ligand to AIM2 [22] containing the ASC domain activated NLRP3-deficient, but not ASC-deficient, THP-1 cells to secrete IL-1β, established target specificity of NPCMD. The precise mechanisms of NLRP3 activation by NPCMD in this study remain unknown. However, inhibition of IL-1β secretion by the endocytosis inhibitor cytochalasin B and a lysosomal enzyme cathepsin B inhibitor, CA-074 Me, suggested involvement of lysosomal rupture and leakage of cathepsin B into the cytosol.

In a recent study, we suggested that NPrCAP can be activated in melanoma cells by tyrosinase leading to the quinone-hapten NPrCAQ, which binds to melanosome or other proteins through their cysteine residues to form possible neo-antigens, thus triggering an immunological response [26]. NPCMD was also oxidized to a quinone form, similar to NPrCAQ (Supplementary Fig. 1). However, the effect of NPCMD to induce cytokine production in monocytes or the monocytic cell line THP-1 is independent of melanosomal oxidation because another analog, NPr (2-*S*) CAP-MIL-CMD, that was not a tyrosinase substrate could induce cytokine production similar to NPr (4-*S*) CAP-MIL-CMD (NPCMD).

Supplementary material related to this article can be found, in the online version, at http://dx.doi.org/10.1016/j.jdermsci.2013.11.006.

Several mechanisms of NLRP3 inflammasome activation have been studied extensively. First, extracellular ATP stimulates the purinergic $P2X_7$ receptors, triggering potassium efflux and inducing recruitment of the pannexin-1 membrane pore [27]. Pore formation allows extracellular NLRP3 agonists to enter into

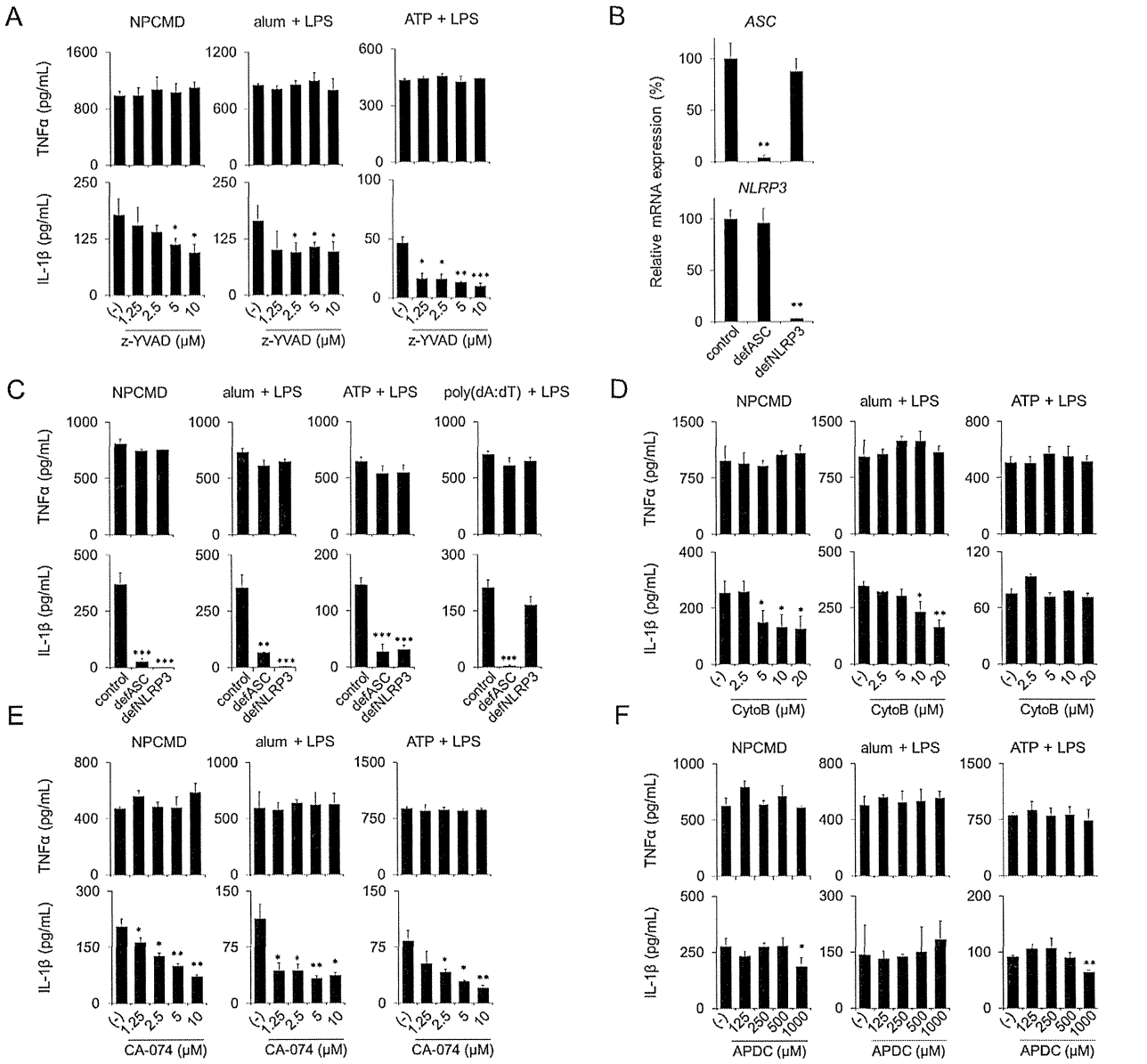

Fig. 3. Involvement of NLRP3 inflammasome activation in IL-1β release from THP-1 cells treated with NPCMD. (A) THP-1 cells (1×10^5) were treated with NPCMD (containing 200 μM NPrCAP), alum (25 μg/mL) plus LPS (50 pg/mL) or ATP (1 μM) plus LPS (50 pg/mL) in the presence of the indicated amounts of z-YVAD-fmk for 18 h. (B) The mRNA levels of ASC and NLRP3 in THP-1 cells (control), ASC-deficient THP-1 cells (defASC) and NLRP3-deficient THP-1 cells (defNLRP3) were quantified by real-time RT-PCR. The percentage of mRNA expression was calculated relative to control cells. (C) THP-1 cells (control), ASC-deficient THP-1 cells (defASC) and NLRP3-deficient THP-1 cells (defNLRP3) (1×10^5 cells) were treated with NPCMD (containing 200 μM NPrCAP), alum (25 μg/mL) plus LPS (50 pg/mL), ATP (1 μM) plus LPS (50 pg/mL), or poly (dA:dT) (10 μg/mL) plus LPS (50 pg/mL) for 18 h. THP-1 cells (1×10^5) were treated with NPCMD (containing 200 μM NPrCAP), alum (25 μg/mL) plus LPS (50 pg/mL) or ATP (1 μM) plus LPS (50 pg/mL) in the presence of the indicated amounts of cytochalasin B (CytoB) in (D), CA-074 Me in (E) or APDC in (F) for 18 h. TNFα and IL-1β in the supernatants were determined by ELISA. The assays were done in triplicate and the values represent the mean ± S.D. Statistical analyses were performed with the Student's *t* test; $^*P < 0.05$, $^{**}P < 0.01$, $^{***}P < 0.001$.

the cytosol and activate NLRP3. Second, some crystallized structures such as MSU, silica, asbestos, and alum have been shown to activate the NLRP3 inflammasome [28,29]. Following endocytosis of these materials, the lysosome ruptured, resulting in leakage of lysosomal contents which activated the NLRP3 inflammasome. The lysosomal protease cathepsin B has been suggested to be a direct ligand for NLRP3 [30]. Third, ROS generated from NLRP3 agonists could be a direct mediator of NLRP3 activation [31,32]. ROS are commonly produced in response to infection or injury. NPCMD caused apoptosis of melanoma cell lines and produced ROS in those cells (data not shown). However, in the present study, NPCMD showed no cytotoxicity to THP-1 cells and the ROS inhibitor APDC inhibited IL-1β secretion from THP-1 cells only marginally. These findings suggest that the involvement of ROS in NPCMD treatment in THP-1 cells is unlikely. However, ROS production following NPCMD treatment in THP-1 cells remains to be clarified.

It was shown that NLRP3 inflammasome activation in DCs induced IL-1β-dependent adaptive immunity against tumors [33–35]. It was also shown that dying tumor cells release ATP, which then acts on $P2X_7$ receptors on DCs and triggers NLRP3 activation, allowing the secretion of IL-1β [34]. The priming of IFNγ-producing CD8 T-cells by dying tumor cells fails in the absence of a functional IL-1 receptor and in Nlrp3-deficient mice. On the other hand, it was shown that antigen-independent responses can be elicited in memory CD8 T-cells by TLR [36] and inflammasome [16] activation. Kupz et al. [16] showed that activation of the NLRC4 inflammasome in dendritic cells by sensing bacterial flagellin caused IFNγ

production by memory CD8 T-cells, mainly by IL-18, and indicated the importance of regulation of non-cognate memory T-cell responses in bacterial immunity. The findings suggest the usefulness of NPCMD as an immunopotentiating agent in combined use with an immunogenic target. Especially, in melanoma, both a direct cytotoxic effect and an NLRP3-mediated immunopotentiating effect are likely to occur with NPCMD. The therapeutic effect of NPCMD in melanoma should be studied. The adjuvant effect of NPCMD to potentiate immunogenicity of cancer/testis antigens is now being investigated in mice.

Source of funding

This work was supported in part by a Health and Labor Sciences Research Grant-in-Aid for Research on Advanced Medical Technology from the Ministry of Health, Labor and Welfare of Japan.

Acknowledgements

We thank Ms. Junko Mizuuchi for preparation of the manuscript. We also thank Dr. Makoto Ojika of Nagoya University for the measurement of ^{1}H-NMR.

References

[1] Ito S, Wakamatsu K. Chemistry of mixed melanogenesis – pivotal roles of dopaquinone. Photochem Photobiol 2008;84:582–92.
[2] Prota G. Regulatory mechanisms of melanogenesis: beyond the tyrosinase concept. J Invest Dermatol 1993;100:156S–61S.
[3] Boissy RE, Manga P. On the etiology of contact/occupational vitiligo. Pigment Cell Res 2004;17:208–14.
[4] Jimbow K, Obata H, Pathak MA, Fitzpatrick TB. Mechanism of depigmentation by hydroquinone. J Invest Dermatol 1974;62:436–49.
[5] Nordlund JJ, Forget B, Kirkwood J, Lerner AB. Dermatitis produced by applications of monobenzone in patients with active vitiligo. Arch Dermatol 1985;121:1141–4.
[6] van den Boorn JG, Picavet DI, van Swieten PF, van Veen HA, Konijnenberg D, van Veelen PA, et al. Skin-depigmenting agent monobenzone induces potent T-cell autoimmunity toward pigmented cells by tyrosinase haptenation and melanosome autophagy. J Invest Dermatol 2011;131:1240–51.
[7] Hariharan V, Klarquist J, Reust MJ, Koshoffer A, McKee MD, Boissy RE, et al. Monobenzyl ether of hydroquinone and 4-tertiary butyl phenol activate markedly different physiological responses in melanocytes: relevance to skin depigmentation. J Invest Dermatol 2010;130:211–20.
[8] Ito S, Kato T, Ishikawa K, Kasuga T, Jimbow K. Mechanism of selective toxicity of 4-S-cysteinylphenol and 4-S-cysteaminylphenol to melanocytes. Biochem Pharmacol 1987;36:2007–11.
[9] Tandon M, Thomas PD, Shokravi M, Singh S, Samra S, Chang D, et al. Synthesis and antitumour effect of the melanogenesis-based antimelanoma agent *N*-propionyl-4-*S*-cysteaminylphenol. Biochem Pharmacol 1998;55:2023–9.
[10] Alena F, Iwashina T, Gili A, Jimbow K. Selective in vivo accumulation of *N*-acetyl-4-*S*-cysteaminylphenol in B16F10 murine melanoma and enhancement of its in vitro and in vivo antimelanoma effect by combination of buthionine sulfoximine. Cancer Res 1994;54:2661–6.
[11] Thomas PD, Kishi H, Cao H, Ota M, Yamashita T, Singh S, et al. Selective incorporation and specific cytocidal effect as the cellular basis for the antimelanoma action of sulphur containing tyrosine analogs. J Invest Dermatol 1999;113:928–34.
[12] Ishii-Osai Y, Yamashita T, Tamura Y, Sato N, Ito A, Honda H, et al. *N*-propionyl-4-*S*-cysteaminylphenol induces apoptosis in B16F1 cells and mediates tumor-specific T-cell immune responses in a mouse melanoma model. J Dermatol Sci 2012;67:51–60.
[13] Schroder K, Tschopp J. The inflammasomes. Cell 2010;140:821–32.
[14] Berg RE, Crossley E, Murray S, Forman J. Memory CD8+ T cells provide innate immune protection against *Listeria* monocytogenes in the absence of cognate antigen. J Exp Med 2003;198:1583–93.
[15] Bou Ghanem EN, McElroy DS, D'Orazio SE. Multiple mechanisms contribute to the robust rapid gamma interferon response by CD8+ T cells during *Listeria* monocytogenes infection. Infect Immun 2009;77:1492–501.
[16] Kupz A, Guarda G, Gebhardt T, Sander LE, Short KR, Diavatopoulos DA, et al. NLRC4 inflammasomes in dendritic cells regulate noncognate effector function by memory CD8(+) T cells. Nat Immunol 2012;13:162–9.
[17] Padgette SR, Herman HH, Han JH, Pollock SH, May SW. Antihypertensive activities of phenyl aminoethyl sulfides, a class of synthetic substrates for dopamine beta-hydroxylase. J Med Chem 1984;27:1354–7.
[18] Prezioso JA, Epperly MW, Wang N, Bloomer WD. Effects of tyrosinase activity on the cytotoxicity of 4-*S*-cysteaminylphenol and *N*-acetyl-4-*S*-cysteaminylphenol in melanoma cells. Cancer Lett 1992;63:73–9.
[19] Sato M, Yamashita T, Ohkura M, Osai Y, Sato A, Takada T, et al. *N*-propionyl-cysteaminylphenol-magnetite conjugate (NPrCAP/M) is a nanoparticle for the targeted growth suppression of melanoma cells. J Invest Dermatol 2009;129:2233–41.
[20] Eisenbarth SC, Colegio OR, O'Connor W, Sutterwala FS, Flavell RA. Crucial role for the Nalp3 inflammasome in the immunostimulatory properties of aluminium adjuvants. Nature 2008;453:1122–6.
[21] Mariathasan S, Weiss DS, Newton K, McBride J, O'Rourke K, Roose-Girma M, et al. Cryopyrin activates the inflammasome in response to toxins and ATP. Nature 2006;440:228–32.
[22] Jones JW, Kayagaki N, Broz P, Henry T, Newton K, O'Rourke K, et al. Absent in melanoma 2 is required for innate immune recognition of Francisella tularensis. Proc Natl Acad Sci U S A 2010;107:9771–6.
[23] Dinarello CA. Interleukin-1 beta, interleukin-18, and the interleukin-1 beta converting enzyme. Ann N Y Acad Sci 1998;856:1–11.
[24] Tschopp J, Schroder K. NLRP3 inflammasome activation: the convergence of multiple signalling pathways on ROS production? Nat Rev Immunol 2010;10:210–5.
[25] Hausmann MJ, Yulzari R, Lewis E, Saisky Y, Douvdevani A. Gel clot LAL assay in the initial management of peritoneal dialysis patients with peritonitis: a retrospective study. Nephrol Dial Transplant 2000;15:680–3.
[26] Ito S, Nishigaki A, Ishii-Osai Y, Ojika M, Wakamatsu K, Yamashita T, et al. Mechanism of putative neo-antigen formation from *N*-propionyl-4-*S*-cysteaminylphenol, a tyrosinase substrate, in melanoma models. Biochem Pharmacol 2012;84:646–53.
[27] Kanneganti TD, Lamkanfi M, Kim YG, Chen G, Park JH, Franchi L, et al. Pannexin-1-mediated recognition of bacterial molecules activates the cryopyrin inflammasome independent of toll-like receptor signaling. Immunity 2007;26:433–43.
[28] Halle A, Hornung V, Petzold GC, Stewart CR, Monks BG, Reinheckel T, et al. The NALP3 inflammasome is involved in the innate immune response to amyloid-beta. Nat Immunol 2008;9:857–65.
[29] Hornung V, Bauernfeind F, Halle A, Samstad EO, Kono H, Rock KL, et al. Silica crystals and aluminum salts activate the NALP3 inflammasome through phagosomal destabilization. Nat Immunol 2008;9:847–56.
[30] Bruchard M, Mignot G, Derangere V, Chalmin F, Chevriaux A, Vegran F, et al. Chemotherapy-triggered cathepsin B release in myeloid-derived suppressor cells activates the Nlrp3 inflammasome and promotes tumor growth. Nat Med 2013;19:57–64.
[31] Cassel SL, Eisenbarth SC, Iyer SS, Sadler JJ, Colegio OR, Tephly LA, et al. The Nalp3 inflammasome is essential for the development of silicosis. Proc Natl Acad Sci U S A 2008;105:9035–40.
[32] Dostert C, Petrilli V, Van Bruggen R, Steele C, Mossman BT, Tschopp J. Innate immune activation through Nalp3 inflammasome sensing of asbestos and silica. Science 2008;320:674–7.
[33] Allen IC, TeKippe EM, Woodford RM, Uronis JM, Holl EK, Rogers AB, et al. The NLRP3 inflammasome functions as a negative regulator of tumorigenesis during colitis-associated cancer. J Exp Med 2010;207:1045–56.
[34] Ghiringhelli F, Apetoh L, Tesniere A, Aymeric L, Ma Y, Ortiz C, et al. Activation of the NLRP3 inflammasome in dendritic cells induces IL-1beta-dependent adaptive immunity against tumors. Nat Med 2009;15:1170–8.
[35] Stagg J, Smyth MJ. Extracellular adenosine triphosphate and adenosine in cancer. Oncogene 2010;29:5346–58.
[36] Tough DF, Sun S, Sprent J. T cell stimulation in vivo by lipopolysaccharide (LPS). J Exp Med 1997;185:2089–94.

Vaccine 32 (2014) 957–964

Contents lists available at ScienceDirect

Vaccine

journal homepage: www.elsevier.com/locate/vaccine

Production of NY-ESO-1 peptide/DRB1*08:03 tetramers and ex vivo detection of CD4 T-cell responses in vaccinated cancer patients

Yu Mizote[a,b], Akiko Uenaka[c], Midori Isobe[b], Hisashi Wada[d], Kazuhiro Kakimi[e], Takashi Saika[f], Shoichi Kita[g], Yukari Koide[g], Mikio Oka[b], Eiichi Nakayama[c,*]

[a] Department of Immunology, Okayama University Graduate School of Medicine, Dentistry and Pharmaceutical Sciences, Okayama, Japan
[b] Department of Respiratory Medicine, Kawasaki Medical School, Okayama, Japan
[c] Faculty of Health and Welfare, Kawasaki University of Medical Welfare, Kurashiki 701-0193, Okayama, Japan
[d] Department of Surgery, Osaka University Graduate School of Medicine, Osaka, Japan
[e] Department of Immunotherapeutics, University of Tokyo Hospital, Tokyo, Japan
[f] Department of Urology, Okayama University Graduate School of Medicine, Dentistry and Pharmaceutical Sciences, Okayama, Japan
[g] Medical & Biological Laboratories, Nagano, Japan

ARTICLE INFO

Article history:
Received 27 June 2013
Received in revised form 17 October 2013
Accepted 18 December 2013
Available online 5 January 2014

Keywords:
Tumor immunology
NY-ESO-1
CD4 T-cell
MHC class II tetramer

ABSTRACT

We established CD4 T-cell clones, Mz-1B7, and Ue-21, which recognized the NY-ESO-1 121–138 peptide from peripheral blood mononuclear cells (PBMCs) of an esophageal cancer patient, E-2, immunized with an NY-ESO-1 protein and determined the NY-ESO-1 minimal epitopes. Minimal peptides recognized by Mz-1B7 and Ue-21 were NY-ESO-1 125–134 and 124–134, respectively, both in restriction to DRB1*08:03. Using a longer peptide, 122–135, and five other related peptides, including either of the minimal epitopes recognized by the CD4 T-cell clones, we investigated the free peptide/DR recognition on autologous EBV-B cells as APC and peptide/DR tetramer binding. The results showed a discrepancy between them. The tetramers with several peptides recognized by either Mz-1B7 or the Ue-21 CD4 T-cell clone did not bind to the respective clone. On the other hand, unexpected binding of the tetramer with the peptide not recognized by CD4 T-cells was observed. The clone Mz-1B7 did not recognize the free peptide 122–135 on APC, but the peptide 122–135/DRB1*08:03 tetramer bound to the TCR on those cells. The failure of tetramer production and the unexpected tetramer binding could be due to a subtly modified structure of the peptide/DR tetramer from the structure of the free peptide/DR molecule. We also demonstrated that the NY-ESO-1 123–135/DRB1*08:03 tetramer detected ex vivo CD4 T-cell responses in PBMCs from patients after NY-ESO-1 vaccination in immunomonitoring.

1. Introduction

To analyze T-cell immunomonitoring after vaccination, peptide/MHC tetramers have become widely used [1]. Peptide/MHC tetramers identified and visualized antigen specific T-cells. MHC class I tetramers were originally developed by Altman and Davis [2], and used for various antigens including those of viral or tumor origin [3,4]. However, MHC class II tetramers have been used in only a few studies because of the difficulty in preparation [5]. The soluble form of MHC class II molecules is necessary to produce tetramers. However, production of such molecules using extracellular domains of MHC class II α and β chains is generally difficult because of a lack of assembly or aggregation [6]. These findings indicate the necessity of transmembrane regions for the proper assembly of the molecules. Kalandadze et al. [7] found that replacement of the hydrophobic transmembrane regions by the Fos and Jun leucine zipper dimerization motifs resulted in the assembly and secretion of DRαβ heterodimers in yeast. Novak et al. [8] developed MHC class II tetramers using DR molecules incorporating leucin zipper motifs to stabilize the DRα and β heterodimer. The procedure has been widely used, but successful production of MHC class II tetramers is still limited [9–13].

We recently analyzed CD4 T-cell responses against NY-ESO-1 in PBMCs from patients who were vaccinated with a complex of cholesterol-bearing hydrophobized pullulan and NY-ESO-1 protein (CHP-NY-ESO-1) in our clinical trial and determined three novel NY-ESO-1 CD4 T-cell epitopes: NY-ESO-1 87–100 bound to DRB1*09:01, NY-ESO-1 95–107 bound to DQB1*04:01, and NY-ESO-1 124–134 bound to DRB1*08:03 [14]. CD4 T-cells that

Abbreviations: APC, antigen-presenting cell; CHP-NY-ESO-1, complex of cholesterol-bearing hydrophobized pullulan and NY-ESO-1 whole protein; Fmoc, *N*-(9-fluorenyl)-methoxycarbonyl; HD, healthy donor; MFI, mean fluorescence intensity; OLP, overlapping peptide; PBMC, peripheral blood mononuclear cell.

* Corresponding author. Tel.: +81 86 462 1111x54954; fax: +81 86 464 1109.
E-mail address: nakayama@mw.kawasaki-m.ac.jp (E. Nakayama).

0264-410X/$ – see front matter © 2013 Elsevier Ltd. All rights reserved.
http://dx.doi.org/10.1016/j.vaccine.2013.12.042

recognized these epitope peptides also recognized EBV-B cells or DC that were treated with recombinant NY-ESO-1 protein or an NY-ESO-1-expressing tumor cell lysate, suggesting that the epitope peptides are naturally processed. These CD4 T-cells had a cytokine profile with Th1 characteristics.

In this study, we showed that tetramers with several peptides recognized by the CD4 T-cell clones did not bind to the same clones. On the other hand, unexpected binding of the tetramer with a peptide not recognized by CD4 T-cells was observed. The failure of tetramer production and the unexpected tetramer binding could be due to a subtly modified structure of the peptide/DR tetramer from the structure of the free peptide/DR molecule. We also demonstrated that the NY-ESO-1 123–135/DRB1*08:03 tetramer detected ex vivo CD4 T-cell responses in PBMCs from patients after NY-ESO-1 vaccination in immunomonitoring.

2. Materials and methods

2.1. Patients and blood samples

Peripheral blood samples were drawn from esophageal cancer patients E-1 and E-2, and a prostate cancer patient P-3, who were vaccinated with CHP-NY-ESO-1, and a lung cancer patient TK-OLP-01, who was vaccinated with NY-ESO-1 OLP in our clinical trials [15,16] after obtaining written informed consent. PBMCs were isolated by density gradient centrifugation using Histopaque 1077 (Sigma–Aldrich, St. Louis, MO). CD4 T-cells and $CD19^+$ cells were purified from PBMCs using CD4 and CD19 microbeads, respectively, using a large scale column and a magnetic device (Miltenyi Biotec, Auburn, CA). The cells were stored in liquid N_2 until use. HLA typing was done using PBMCs with a sequence-specific oligo-nucleotide probe and sequence-specific priming of genomic DNA using standard procedures. Patient E-2 was found to possess homozygous alleles.

2.2. Peptides

Peptides were synthesized using standard solid-phase methods based on *N*-(9-fluorenyl)-methoxycarbonyl (Fmoc) chemistry on a Multiple Peptide Synthesizer (AMS422, ABIMED, Langenfeld, Germany) at Okayama University (Okayama, Japan).

2.3. Cell lines

E-2 bulk CD4 T-cells were stimulated in vitro twice as described previously [14]. Clones were then established by limiting dilution. EBV-B cells were generated from $CD19^+$ peripheral blood B cells using the culture supernatant from EBV-producing B95-8 cells.

2.4. Generation of HLA-DRB1*08:03 tetramers

HLA-DR tetramers were prepared as described previously [5]. The cDNA coding for the extracellular domains of the HLA-DRα chain was inserted by fusion PCR in a basic leucine zipper and His tag. The HLA-DRβ chain was fused with an acidic leucine zipper and the BirA substrate peptide for BirA enzyme-dependent biotinylation. The HLA-DRα and HLA-DRβ chimeric cDNA were cloned into the pcDNA3.1 vector, respectively. The expression vectors containing the HLA-DRα and HLA-DRβ chains were co-transfected into CHO cells.

2.5. ELISA

Supernatants (100 μl) from cultures of CD4 T-cells (5×10^3) stimulated for 18 h with autologous EBV-B cells (5×10^3) pre-pulsed for 30 min with peptide in a 96-well round bottomed culture plate, or with solid-phase peptide/HLA-DRB1*08:03 tetramers in a 96-well flat bottomed culture plate, were collected and the amounts of IFNγ were estimated by sandwich ELISA [14]. TNFα, IL-4, IL-10 and IL-17A in the culture supernatants were estimated by DuoSet Sandwich ELISAs (R&D Systems, Minneapolis, MN), according to the manufacturer's instructions.

2.6. Flow cytometry

FITC-conjugated anti-human TCRαβ mAb (BD), PerCP Cy5.5-conjugated anti-human CD3 mAb and APC-conjugated anti-human CD4 mAb (eBioscience, San Diego, CA) were used for T-cell surface staining. The stained cells were detected by FACS Canto II (BD). Flow cytometry results were analyzed with FlowJo (Tree Star, Ashland, OR).

2.7. Tetramer staining

CD4 T-cells were incubated with tetramers for 1 h at 37 °C in a 5% CO_2 atmosphere. FITC-conjugated anti-human CD4 mAb (Miltenyi Biotec) was added at the end of tetramer staining and incubated for an additional 20 min at 4 °C.

2.8. IFNγ capture assay

The method has been described previously [14].

2.9. TCR Vβ and CDR3 sequence analysis

For TCR Vβ analysis, the IOTest Beta Mark kit (Beckman Coulter, Brea, CA) was used. The CDR3 sequence was determined by PCR as described previously [17].

3. Results

3.1. Determination of NY-ESO-1 minimal epitopes recognized by CD4 T-cell clones Mz-1B7 and Ue-21 established from PBMCs of an esophageal cancer patient E-2 immunized with CHP-NY-ESO-1

We established CD4 T-cell clones from PBMCs of an esophageal cancer patient E-2 immunized with CHP-NY-ESO-1 which recognized the 18-mer NY-ESO-1 121–138 peptide. The CD4 T-cell clones Mz-1B7 and Ue-21 produced IFNγ, TNFα, but not IL-4, IL-10 or IL-17A (Supplementary Fig. 1), indicating that they have Th1 characteristics. We determined restriction molecules by antibody blocking and minimal epitopes using various N- and C-termini truncated peptides. Assays were done by ELISA examining IFNγ in the culture supernatant from responding T-cells using autologous EBV-B cells as antigen-presenting cells (APC). As shown in Fig. 1A, recognition of the 18-mer NY-ESO-1 121–138 by CD4 T-cell clones Mz-1B7 and Ue-21 was inhibited by addition of anti-HLA-DR mAb, but not anti-HLA-DQ mAb. Since patient E-2 possessed homozygous haplotypes (DRB1*08:03, DQA1*01:03, DQB1*06:01, DPB1*05:01) according to genetic analysis (see Section 2), the two clones Mz-1B7 and Ue-21 recognized the NY-ESO-1 peptide 121–138 in restriction to DRB1*08:03.

We then investigated recognition of various N- and C-termini truncated peptides and found that a core peptide region recognized by either clone Mz-1B7 or clone Ue-21 was made up of amino acids 125–134 (Fig. 1B). Further analysis revealed that a minimal peptide recognized by clone Mz-1B7 was peptide 125–134 (10-mer) and that recognized by clone Ue-21 was peptide 124–134 (11-mer) (Fig. 1C). Thus, clones Mz-1B7 and Ue-21 recognized

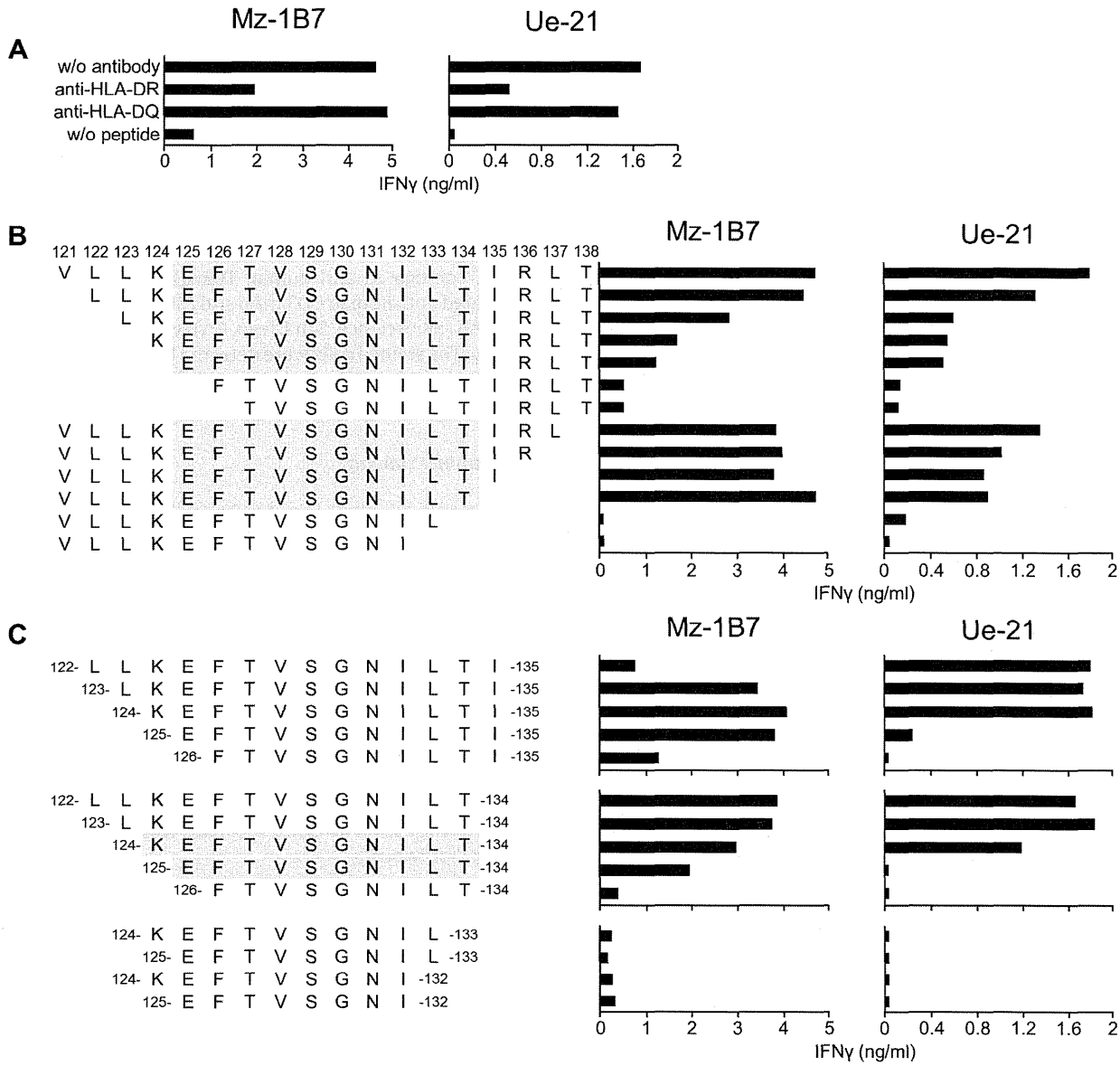

Fig. 1. Antibody blocking (A) and determination of NY-ESO-1 minimal epitopes ((B) and (C)) recognized by E-2 CD4 T-cell clones Mz-1B7 and Ue-21. In (A), CD4 T-cell clones (5×10^3) were stimulated for 18 h with autologous EBV-B cells (5×10^3) in the presence of NY-ESO-1 121–138 (VLLKEFTVSGNILTIRLT) peptide (100 nM), and anti-HLA-DR or anti-HLA-DQ mAb (5 μg/ml) in the culture. IFNγ in the culture supernatants was determined by ELISA. In B and C, CD4 T-cell clones (5×10^3) were stimulated for 18 h with autologous EBV-B cells (5×10^3) in the presence of truncated NY-ESO-1 121–138 peptides (100 nM). The core peptide region and each minimal epitopes recognized by CD4 T-cell clones are shown in gray boxes. IFNγ in the culture supernatants was determined by ELISA.

closely related, but different, minimal NY-ESO-1 peptides in restriction to the same DRB1*08:03. Recognition of closely related, but different, peptides by these CD4 T-cell clones was further confirmed with responses to other peptides. Peptide 122–135 was recognized by Ue-21, but not Mz-1B7. On the other hand, peptide 125–135 and peptide 126–135 were recognized by Mz-1B7, but not Ue-21.

3.2. Differential recognition by clone Mz-1B7 and clone Ue-21 of the longer peptide 122–135, including minimal epitopes recognized by either clone

To confirm that the longer peptide 122–135 was recognized by only clone Ue-21, but not clone Mz-1B7, irrespective of including epitopes recognized by either clone, an IFNγ capture assay together with ELISA was performed examining IFNγ in the same culture stimulated with peptide 122–135 and five other related peptides using autologous EBV-B cells as APC as above. As shown in Fig. 2A, a response of clone Mz-1B7 was observed against the peptides 123–135, 124–135, 122–134, 123–134 and 124–134, but not 122–135 in either the IFNγ capture assay or ELISA. No response against peptide 122–135 was observed up to a peptide concentration of 100 nM in ELISA. On the other hand, a response of clone Ue-21 was observed against all of the peptides used. These results were consistent with the results shown in Fig. 1.

3.3. Tetramer binding

We produced tetramers using the longer peptide 122–135, and five other related peptides 123–135, 124–135, 122–134, 123–134 and 124–134. The DR molecule was constructed by combining the DRA*01:01 and DRB1*08:03 chains that fused the leucine zipper motif at the C-terminal ends [8]. In the DRA locus, seven alleles DRA*01:01:01:01, DRA*01:01:01:02,

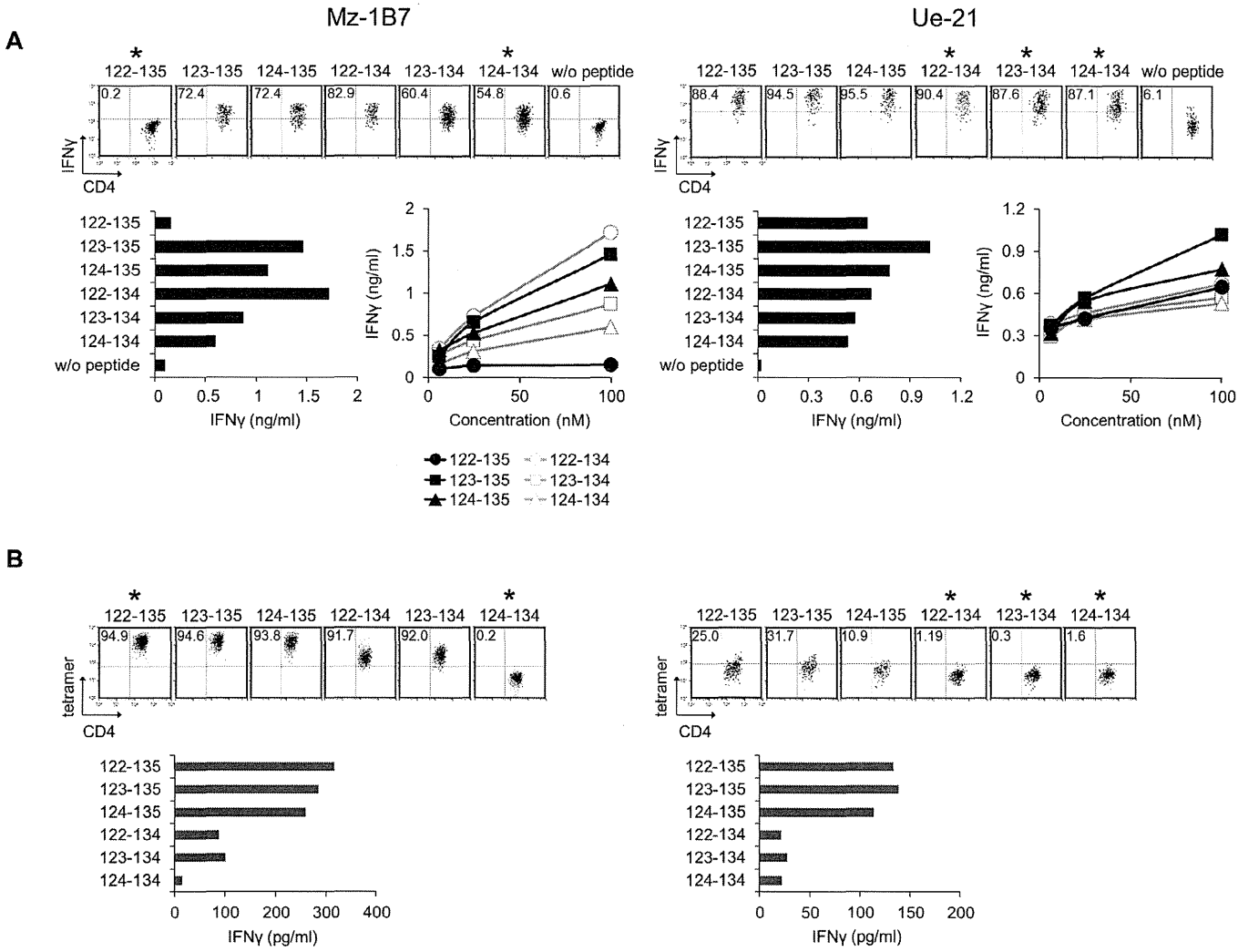

Fig. 2. Discrepancy between peptide recognition (A) and tetramer binding (B) in E-2 CD4 T-cell clones Mz-1B7 and Ue-21. In A top, CD4 T-cell clones (1×10^4) were stimulated for 4 h with the indicated peptides (1 μM) using autologous EBV-B cells (1×10^4) as APC. IFNγ-secreting CD4 T-cells were determined by an IFNγ capture assay using FACS Canto II. In A bottom, CD4 T-cell clones (5×10^3) were stimulated for 18 h with autologous EBV-B cells (5×10^3) pre-pulsed for 30 min with the indicated peptides (100 nM) (left) or with graded concentrations (6.25, 25 or 100 nM) of the indicated peptides (right). IFNγ in the culture supernatant was determined by ELISA. In B top, CD4 T-cell clones were stained with the indicated peptide/HLA-DRB1*08:03 tetramers (5 μg/ml) at 37 °C for 1 h followed by staining with an anti-CD4 mAb, and analyzed using FACS Canto II. In B bottom, CD4 T-cell clones (5×10^3) were stimulated for 18 h with the indicated peptide/HLA-DRB1*08:03 tetramers coated on wells in microculture plates. IFNγ in the culture supernatant was determined by ELISA. The peptides that show a discrepancy between recognition (A) and tetramer binding (B) are marked by *.

DRA*01:01:01:03, DRA*01:01:02, DRA*01:02:01, DRA*01:02:02 and DRA*01:02:03 have been identified. These alleles differ only at amino acid 217 in the cytoplasmic domain, which is included in the region replaced by a leucin zipper motif from amino acid residue 152 in the α2 domain. Therefore, any DRA allele can be used for tetramer production.

With these six peptide/DR tetramers, we examined binding to clones Mz-1B7 and Ue-21. As shown in Fig. 2B, to clone Mz-1B7, binding of tetramers with peptide 122–135, 123–135, 124–135, 122–134 and 123–134, but not 124–134, was observed. The peptide 122–135 including the minimal epitope 125–134 was not recognized by Mz-1B7, but a tetramer constructed using the same peptide bound to Mz-1B7. Furthermore, peptide 124–134 that also included the minimal epitope 125–134 was recognized by Mz-1B7, but a tetramer constructed using the same peptide did not bind to the same clone.

On the other hand, to clone Ue-21, weak binding of tetramers with peptides 122–135, 123–135 and 124–135, but only marginal binding of tetramers with 122–134, 123–134 or 124–134, was observed. The peptides 122–134 and 123–134, including the minimal epitope 124–134 and the peptide124–134 itself, were recognized by Ue-21, but the tetramers constructed using the same peptides bound to the same clone only marginally. IFNγ production by CD4 T-cell clones in stimulation with the tetramers was consistent with tetramer binding (Fig. 2B bottom).

We further examined the only marginal binding of a tetramer constructed using the peptide 124–134 to Mz-1B7 and Ue-21 under different culture conditions. As shown in Fig. 3A and B, efficient binding of the tetramer constructed using the peptide 123–135 to clone Mz-1B7 was observed at 25–37 °C after incubation for 10–120 min. However, only marginal binding was observed with the tetramer constructed using the peptide 124–134, even at 37 °C after incubation for 120 min. Only marginal binding of the tetramer with the peptide 124–134 to Mz-1B7 or Ue-21 was observed up to a concentration of 10 μg/ml (Fig. 3C and D).

3.4. Expression of CD4 and TCR on CD4 T-cell clones

Expression of CD4, CD3 and TCRαβ was analyzed by FACS. As shown in Fig. 4A, expression of CD4 was observed similarly on clones Mz-1B7 and Ue-21. On the other hand, expression of CD3 and TCRαβ was observed on Ue-21 strongly, but on Mz-1B7

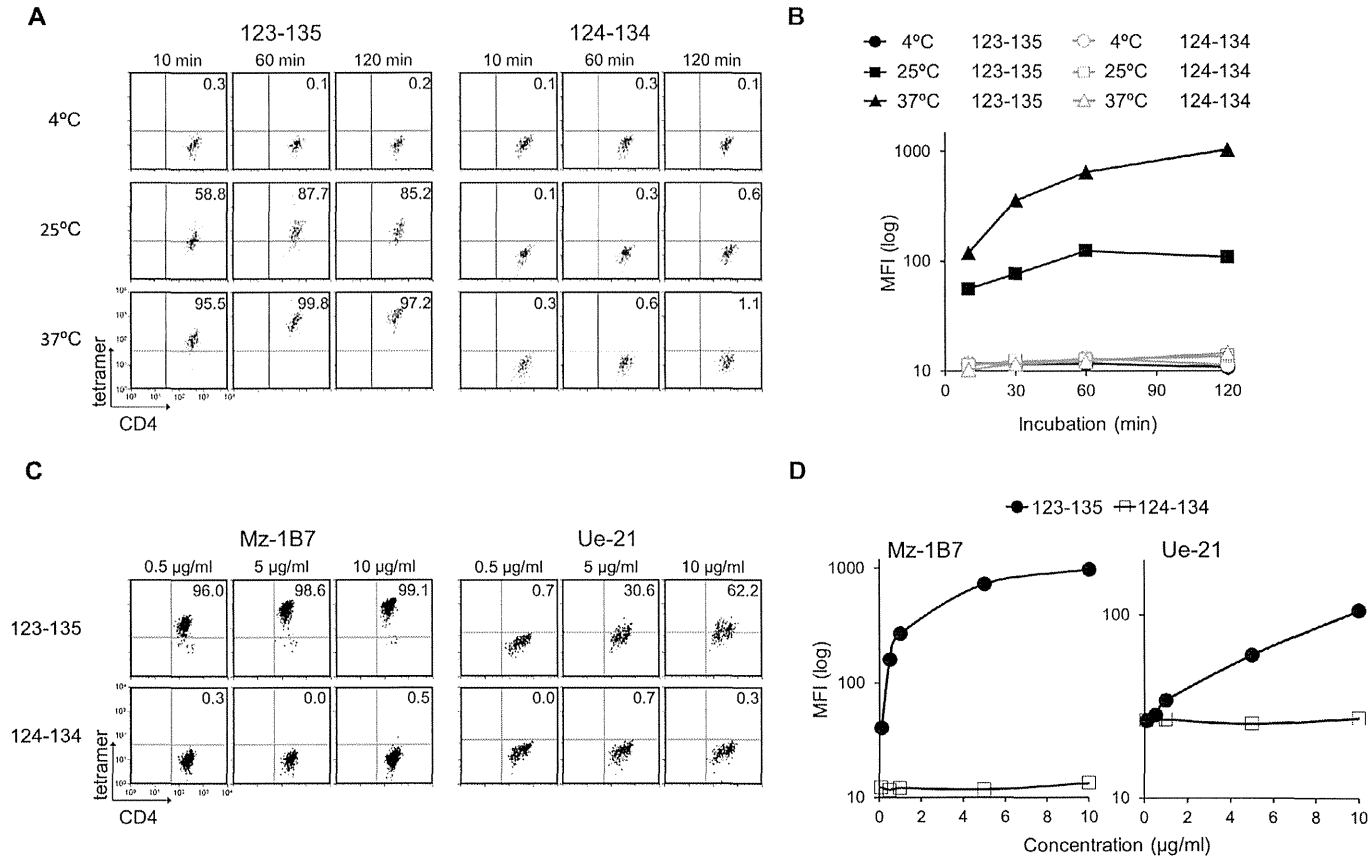

Fig. 3. Effect of temperature, incubation time and dose in tetramer staining. In (A) and (B), the E-2 CD4 T-cell clone Mz-1B7 was stained with NY-ESO-1 123–135 (LKEFTVSGNILTI) or NY-ESO-1 124–134 (KEFTVSGNILT) peptide/HLA-DRB1*08:03 tetramers (5 μg/ml) at 4, 25 or 37 °C for 10, 30, 60 or 120 min followed by staining with anti-CD4 mAb. In C and D, E-2 CD4 T-cell clones Mz-1B7 and Ue-21 were stained with NY-ESO-1 123–135 (LKEFTVSGNILTI) or NY-ESO-1 124–134 (KEFTVSGNILT) peptide/HLA-DRB1*08:03 tetramers (0.5, 1, 5 or 10 μg/ml) at 37 °C for 1 h followed by staining with an anti-CD4 mAb. Analysis was done using FACS Canto II. Dot plots (A and C) and the mean fluorescence intensity (MFI) (B and D) of tetramer staining are shown.

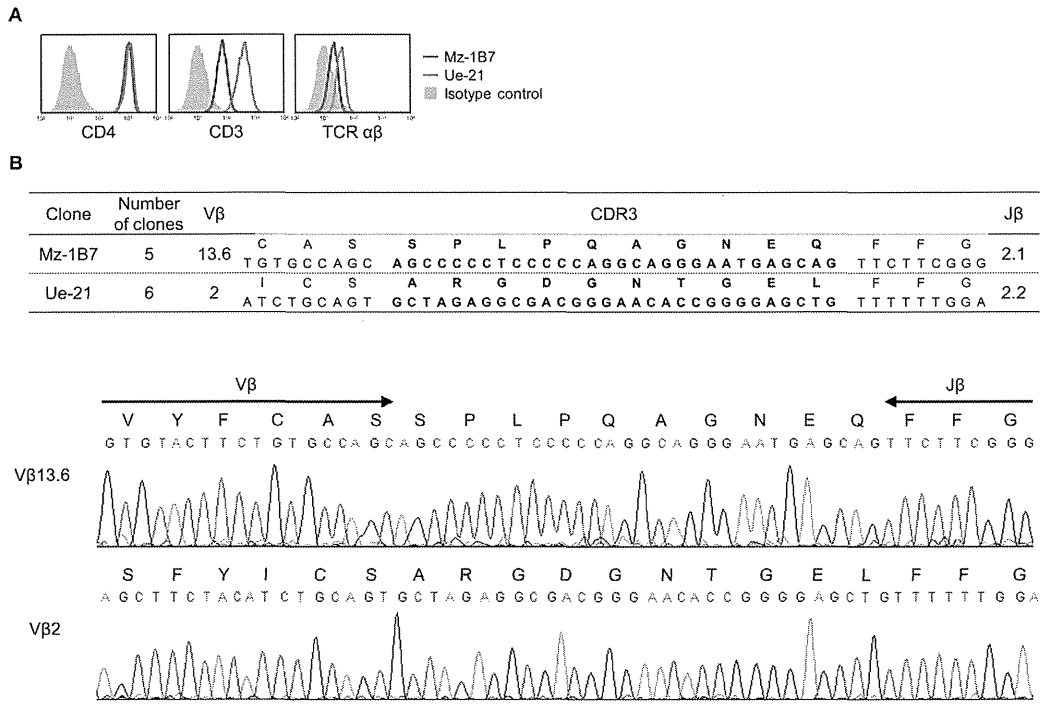

Fig. 4. Surface expression of the molecules on CD4 T-cell clones (A) and analysis of CDR3 sequences (B). In A, CD4 T-cell clones Mz-1B7 and Ue-21 stained with anti-CD4, CD3 and TCRαβ mAb were analyzed using FACS Canto II. In B, the nucleotide sequence and deduced amino acid sequences of the V–D–J junctional region of TCR β chain from the E-2 CD4 T-cell clones are shown.

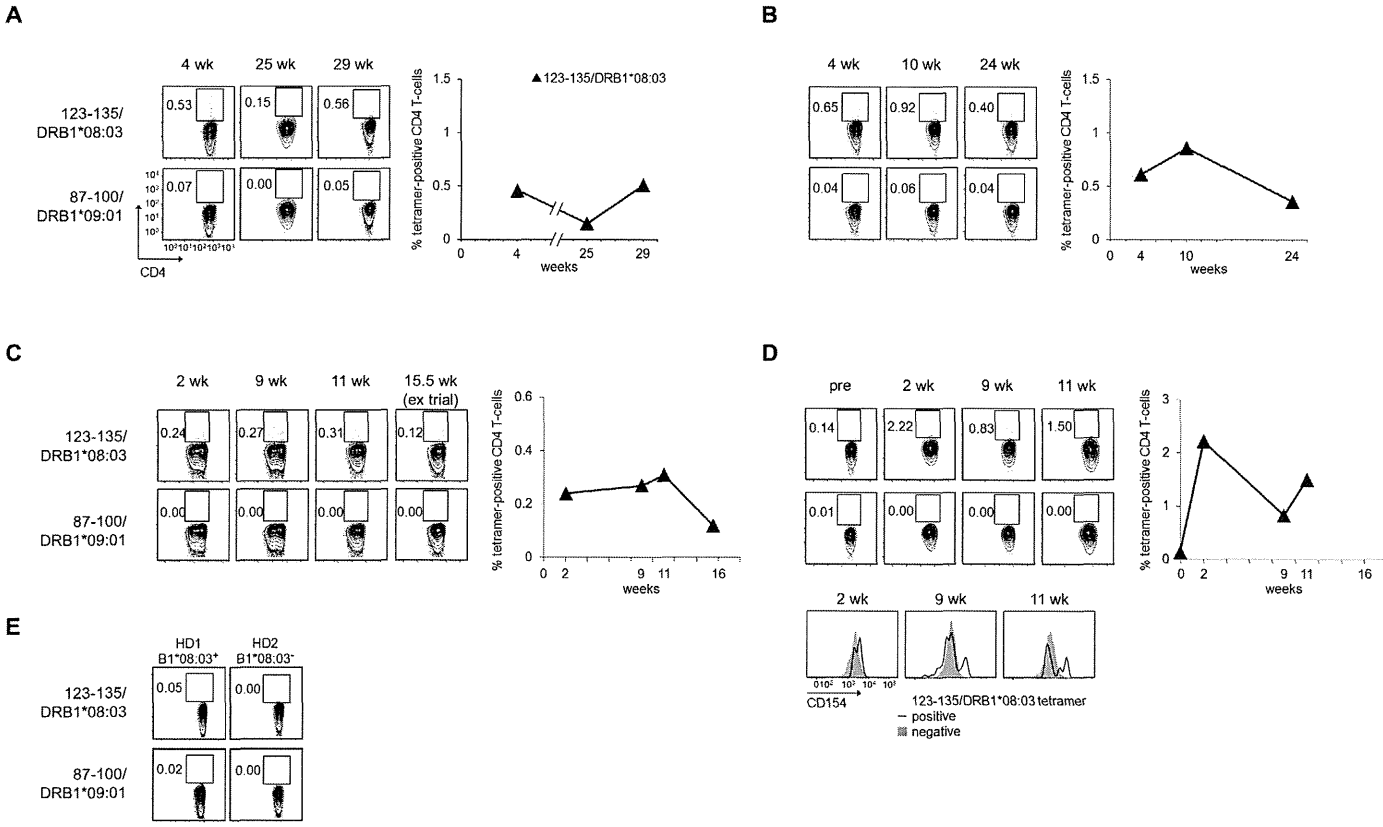

Fig. 5. Immunomonitoring of CD4 T-cell responses by the tetramer in cancer patients immunized with NY-ESO-1. CD4 T-cells from prostate cancer patient P-3 (A) and esophageal cancer patient E-1 (B) who were immunized with CHP-NY-ESO-1, and a lung cancer patient TK-OLP-01 (C) who was immunized with NY-ESO-1 OLP were stained ex vivo with the NY-ESO-1 123–135/HLA-DRB1*08:03 tetramer or a control NY-ESO-1 87–100/HLA-DRB1*09:01 tetramer (5 μg/ml) at 37 °C for 1 h followed by staining with an anti-CD4 mAb. In D, TK-OLP01 CD4 T-cells after in vitro stimulation twice were stained with the NY-ESO-1 123–135/HLA-DRB1*08:03 tetramer or a control NY-ESO-1 87–100/HLA-DRB1*09:01 tetramer and anti-CD154 mAb at 37 °C for 2 h followed by staining with an anti-CD4 mAb. The histogram shows CD154 expression on NY-ESO-1 123–135/DRB1*08:03 tetramer-positive (open) and negative (filled) CD4 T-cells. CD4 T-cells from two HDs were stained with tetramers as a negative control (E). HD1 and HD2 are DRB1*08:03-positive and -negative individuals, respectively. Analysis was done using FACS Canto II.

moderately. As shown in Fig. 4B, analysis of CDR3 sequences revealed that clone Mz-1B7 utilizes the Vβ13.6, SPLPQAGNEQ sequence for CDR3 and Jβ2.1. On the other hand, clone Ue-21 utilizes the Vβ2, ARGDGNTGEL sequence for CDR3 and Jβ2.2.

By cloning bulk CD4 T-cells from the E-2 patient, we obtained 58 DRB1*08:03-restricted clones. Within these, 5 clones utilized Vβ13.6 and 53 clones Vβ2. 5 clones with Vβ13.6 and 6 clones with Vβ2 were sequenced for CDR3. A combination of the same CDR3 sequence and Jβ was utilized by clones with each Vβ, respectively.

3.5. Monitoring of CD4 T-cell response by a tetramer constructed using the peptide 123–135 in cancer patients immunized with NY-ESO-1

Tetramers constructed using the peptide 123–135 (NY-ESO-1 123–135/DRB1*08:03) were used to monitor CD4 T-cell responses in DRB1*08:03-expressing cancer patients immunized with CHP-NY-ESO-1, or a mixture of NY-ESO-1 OLPs (NY-ESO-1 79–108, 100–129, 121–150 and 142–173) with Picibanil and Montanide. As shown in Fig. 5, the tetramer detected positive cells ex vivo in CD4 T-cells from PBMCs of a prostate cancer patient (P-3) (Fig. 5A) and an esophageal cancer patient (E-1) (Fig. 5B) who expressed DRB1*08:03 after immunization with CHP-NY-ESO-1. The tetramer also detected positive cells in CD4 T-cells from PBMCs of a lung cancer patient (TK-OLP-01) immunized with NY-ESO-1 OLP ex vivo (Fig. 5C) and after in vitro stimulation (Fig. 5D). Predominant detection of tetramer NY-ESO-1 123–135/DRB1*08:03-positive cells was observed after in vitro stimulation. Induction of CD154 (CD40L) expression on tetramer-positive cells was examined. At 9 and 11 weeks (3 and 4 vaccinations) after immunization, CD154 (CD40L)-positive cells were detected in tetramer NY-ESO-1 123–135/DRB1*08:03-positive, but not negative, cells suggesting their activation. No tetramer-positive cells were detected in CD4 T-cells from DRB1*08:03-positive or negative healthy donors (HD) (Fig. 5E). No clonal analysis of CD4 T-cells was possible because PBMCs from these patients were not available for further study.

4. Discussion

In this study, we demonstrated that HLA class II tetramers produced using minimal epitope peptides efficiently recognized by CD4 T-cell clones did not bind to cognate CD4 T-cell clones. Furthermore, we showed that a tetramer produced using a peptide which included the epitope sequence, but was not recognized by the cognate CD4 T-cell clone, could bind to the same CD4 T-cell clone.

It has long been observed that production of HLA class II tetramers is extremely difficult when compared to the production of MHC class I tetramers [5,6]. HLA class II tetramers produced using minimal epitope peptides and HLA class II molecules dimerized by a leucine zipper motif incorporated in the molecule generally failed to bind cognate CD4 T-cell clones. There have been only a few reports of successful binding of MHC class II tetramers to CD4 T-cells in which long peptides which were recognized by those T-cells were used for tetramer production [9–11].